UNIVERSITÀ DEGLI STUDI DI NAPOLI

"FEDERICO II"

Scuola di Dottorato in Medicina Molecolare

Dottorato di Ricerca in Genetica e Medicina Molecolare

Functional characterization of the malignant hyperthermia mutation T1354S in the α_{1S} subunit of the skeletal muscle voltage-gated Ca^{2+} channel

Coordinatore:
Prof. Carmelo Bruno Bruni

Candidato:
Dott. Antonella Pirone

Anno
2007

UNIVERSITÀ DEGLI STUDI DI NAPOLI

"FEDERICO II"

Dipartimento di Biochimica e Biotecnologie Mediche
Univeristá degli Studi di Napoli
"Federico II"

Dottorato di Ricerca in Genetica e Medicina Molecolare

Coordinatore Prof. Carmelo Bruno Bruni

Sede amministrativa:
Dipartimento di Biologia e Patologia Cellulare e Molecolare "Luigi Califano"

UNIVERSITÀ DEGLI STUDI DI NAPOLI

"FEDERICO II"

Dipartimento di Biochimica e Biotecnologie Mediche
Univeristá degli Studi di Napoli
"Federico II"

Tesi di Dottorato di Ricerca in Genetica e Medicina Molecolare
XIX ciclo

Functional characterization of the malignant hyperthermia mutation T1354S in the α_{1S} subunit of the skeletal muscle voltage-gated Ca^{2+} channel

Candidato: Dott. Antonella Pirone

Docente guida: Prof. Francesco Salvatore

INTRODUCTION

Skeletal Myotube

Skeletal muscle is exquisitely tailored for skeletal stabilization, force generation and coordinated movement. Unlike most tissues, it does not consist of individual cells; rather it is formed from huge, multinucleate muscle fibers, which develop by fusion forming a syncytium of many individual cells, called myoblasts. For coordinated action the entire fiber contracts together as a single unit. Synchronization of contraction along the length of the fiber is accomplished by the muscle fiber action potential which zips rapidly along the fiber after being triggered by neurotransmitter release at the motor end plate upon arrival of a motor axon action potential. The depolarization signal is transmitted uniformly throughout the cell by means of transverse (or T-) tubules (Fig.1), which are invaginations of the surface plasma membrane closely juxtaposed to the membrane of the sarcoplasmic reticulum (SR). The SR is the Ca^{2+}-storage compartment of the muscle whose membranes are rich in active transport systems, like e.g., the Ca^{2+}-ATPase pump (SERCA), that pumps intracellular Ca^{2+} back into the SR. Around the myofibrils the SR forms a network of longitudinal tubules, with enlarged sacs at its end, called terminal cisternae. The juxtaposition of **two** terminal cisternae of SR and **one** T-tubule creates a functional unit, called the ***triad*** (Fig.1).

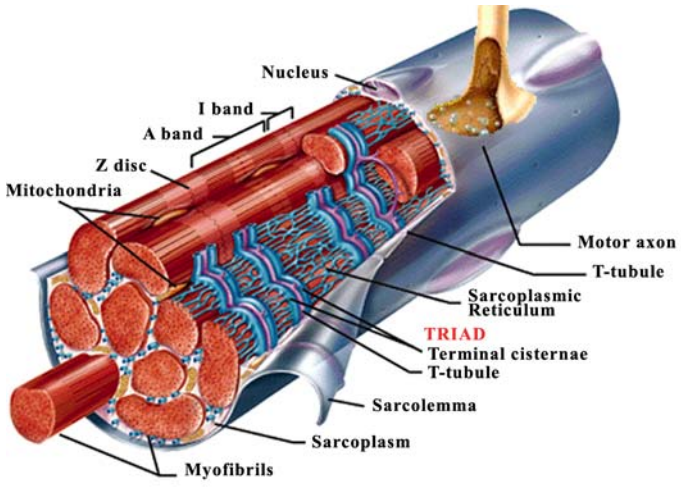

Fig. 1: Skeletal myotube. Action potentials move along the membrane and are transmitted to the entire cell via T-tubules that are closely juxtaposed to the membranes of terminal SR cisternae and thus forming the triads. There, membrane depolarization is converted into muscle-contraction.
Saladin et al. (2004), Anatomy & Physiology: The unit of form and function.

Exactly at the triad the interaction between two distinct Ca^{2+} channels, the voltage-gated L-type Ca^{2+} channel or dihydropyridine receptor (DHPR), located in the T-tubule's plasma membrane and the skeletal muscle Ca^{2+} release channel or ryanodine receptor (RyR1), situated in the SR membrane, mediates the conversion of membrane depolarization into muscle-contraction (excitation-contraction coupling).

Dihydropyridine Receptor (DHPR)

The dihydropyridine receptor DHPR is a voltage-gated L-type Ca^{2+} channel, located in the membrane of the T-tubule, essential in excitation-contraction (EC) coupling [1]. This channel is a multi-subunit complex, composed of a pore-forming α_1 subunit and the auxiliary $\alpha_2\delta$, β and γ subunits (Fig.2).

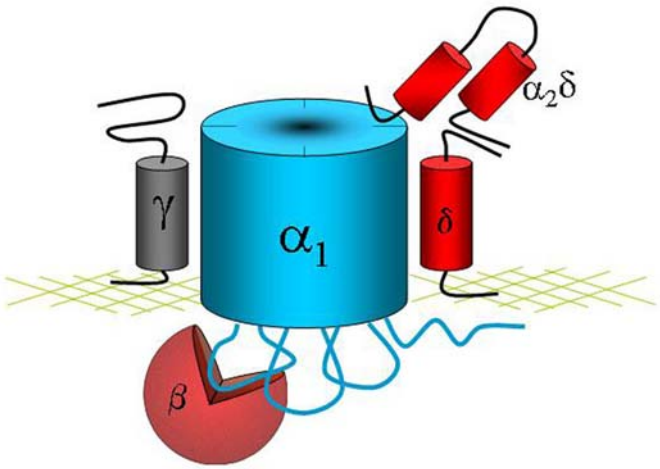

Fig. 2. DHPR. It is a multi-subunits complex. The main subunit α_{1S} acts as pore, gate and voltage-sensor of the channel. It interacts directly with the cytoplasmic β subunit and the two transmembrane/extracellular subunits $\alpha_2\delta$ and γ. These auxiliary subunits modulate the expression and the functions of the Ca^{2+} channel.

The central subunit of the skeletal muscle Ca^{2+} channels is $\alpha_{1S,}$ which acts as voltage-sensor and Ca^{2+} selectivity filter. The α_1 subunit is a protein of 193kDa, resembling in its primary and secondary structure the α subunit of the voltage-gated Na^+ channel (Fig.3).

It consists of four repeated ("homologous") domains (I to IV), each with six transmembrane α-helical segments (S1-S6) and a membrane-associated loop between S5 and S6 (pore loop). Like in other voltage sensitive channels, α_{1S} is gated open and closed by the position of few positive charged residues that move in response to changes in the membrane potential. These charges are localized in the S4 segments of each repeated domain and serve as voltage sensor [2].

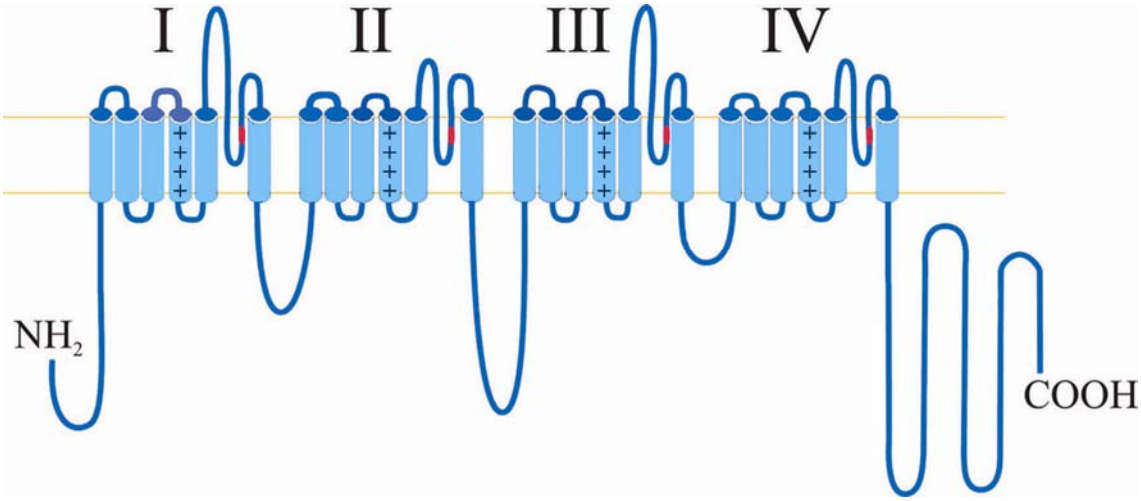

Fig. 3. **The pore-forming subunit of the DHPR**. The α_1 subunit consists of four repeated domains (I-IV), each with six transmembrane segments. The S4 segments are positively charged (+) and function as voltage-sensor of the channel. The four glutamates (red) in the S5-S6 p-loops contribute to the channel selectivity for Ca^{2+} ions. The I-II linker contains the AID sequence motif whereas the II-III linker is responsible for coupling of α_{1S} with RyR.

The channel's selectivity for Ca^{2+} is dependent on the high-affinity binding of Ca^{2+} within the pore. This binding site involves four conserved glutamate residues, in equivalent positions in all the S5-S6 pore loops [3]. The α_{1S} subunit contains binding sites for pharmacological active drugs, the so-called Ca^{2+} channel blockers, phenylalkylamines (PAA), benzothiazepines (BTZ), and 1,4-dihydropyridines (DHP) as well as the molecular domains for interactions with the accessory subunits and with the RyR1. The cytoplasmic linker between the domains I and II contains a conserved motif of nine amino acids, the AID (*Alpha Interaction Domain*) that mediates the interaction between α_1 and β subunits [4, 5]. Another important region of α_{1S} is a short segment of 45 amino acid (residues 720-765) in the II-III linker, that is responsible for

bidirectional-signaling interactions with RyR1[6]. The β subunit is a cytoplasmic protein which interacts with the DHPR complex via BID (*Beta Interaction Domain*) [4]. The β subunit is essential for the development of functional skeletal muscle: its absence eliminates EC coupling and modifies the Ca^{2+} currents in skeletal muscle cells[7]. Schredelseker *et al.* [8]showed that the skeletal muscle β_1 subunit is essential for the skeletal muscle-specific arrangement of DHPR with RyR, a prerequisite for EC coupling. In contrast, the other two auxiliary subunits, $\alpha_2\delta$ and γ are functional modulators of the Ca^{2+} channel. The $\alpha_2\delta$ complex is a disulfide-linked heterodimer, the product of a single gene that is post-translationally cleaved. It is anchored in the T-tubule membrane by a transmembrane segment in the δ subunit and is an important determinant of the kinetic properties of the L-type Ca^{2+} currents [9]. The γ subunit, expressed exclusively in skeletal muscle, is targeted to the surface membrane in the absence of the α_1 but requires the α_1 subunit for its association to the DHPR complex[10] and for the negative modulation of the Ca^{2+} currents [11].

Ryanodine Receptor (RyR)

The ryanodine receptor, is the Ca^{2+} release channel of the SR membrane. There are three different isoforms of RyR (RyR1, RyR2, RyR3), encoded by three different genes. The predominant RyR isoform in skeletal muscle is the RyR1 protein, commonly referred to as the skeletal RyR isoform. RyRs consist of polypeptides of approximately ~560 kDa arranged in a homotetrameric structure with at least two functional domains: a carboxyl-terminal transmembrane domain containing the conduction pore of the Ca^{2+} release channel and a large amino-terminal cytoplasmic domain referred to as the "foot structure" [12]. The activity of the skeletal muscle Ca^{2+} release channel is modulated by a wide spectrum of endogenous and exogenous ligands like Mg^{2+}, ATP, calmodulin, caffeine and it is regulated in a biphasic manner by ryanodine and Ca^{2+}. Low concentrations (nanomolar) of ryanodine activate the channel, whereas high concentrations (>100 μM) inhibit the channel activity. In the same way, the RyR channel is activated by low Ca^{2+} concentrations (1-10 μM) and inhibited by high Ca^{2+} concentrations (1-10 mM). Ca^{2+} regulation plays a role in all RyR-mediated signaling cascades.

While in skeletal muscle the regulating Ca^{2+} signal may amplify RyR1 channel activity only to a limited extent, the Ca^{2+} signal in cardiac muscle even initiates RyR2 channel activity (trigger Ca^{2+}).

Excitation-Contraction Coupling (EC)

The functional interaction between the DHPR and RyR1 is commonly referred to as EC coupling. Depolarization of the T-tubule membrane (*excitation*) induces conformational changes in the DHPR that leads to activation of RyR resulting in a massive Ca^{2+} release from the SR. The transient increase of intracellular Ca^{2+} activates the contractile apparatus of the muscle fibers. The interaction between these two channels in cardiac muscle employs a different mechanism compared with that in skeletal muscle. In cardiac muscle, the L-type channel opens rapidly and generates a large inward influx of Ca^{2+} which induces Ca^{2+} release through the cardiac-type ryanodine receptor (RyR2) - a process called Ca^{2+}-induced Ca^{2+} release (CICR)[13]. In contrast, in skeletal muscle cells Ca^{2+} release is independent of Ca^{2+} influx through DHPR. In fact, the application of Ca^{2+} current blockers does not affect EC coupling [14, 15]. Skeletal muscle DHPR functions predominantly as voltage sensor and activates RyR1 by direct protein-protein interaction[16].

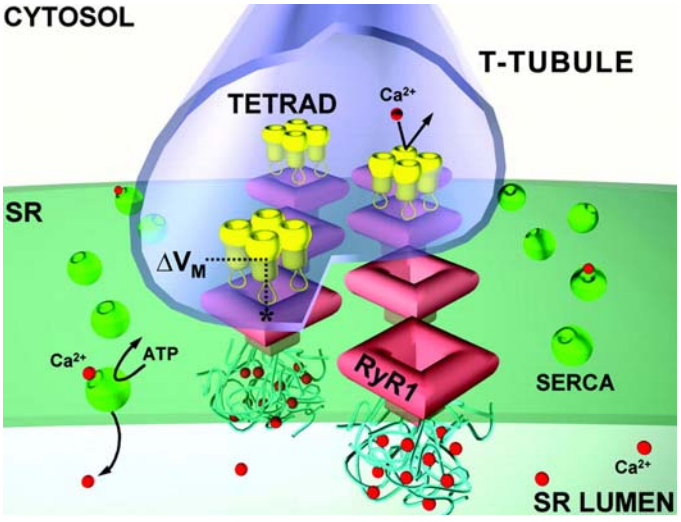

Fig. 4. Skeletal muscle-type EC coupling. In skeletal muscle, DHPR and RyR1 are physically and functionally linked to each other within the junctional domains. The T-tubule contains groups of four DHPRs (tetrads). Every other RyR1 channel is associated with such a DHPR tetrad. Membrane voltage changes (ΔV_M) activate the DHPR and trigger the RyR1 channel to open and release the Ca^{2+} stored inside the sarcoplasmic reticulum (SR) *(from Fill and Copello, 2002)*

The physiological difference in the EC coupling mechanisms in the two muscle types is reflected in the structural arrangements of DHPRs and RyRs in the junctional domains.
In skeletal muscle, four DHPRs are grouped to form a so called tetrad, located in exact correspondence to RyRs [17, 18]. Furthermore RyR1 channels are disposed in orthogonal arrays where every other RyR is associated with a DHPR tetrad. This arrangement is indicative of the physical coupling between DHPRs and RyRs, a feature indispensable for the Ca^{2+}- independent skeletal-type EC coupling [19].

Malignant Hyperthermia

Abnormalities in Ca^{2+} regulatory proteins can lead to different muscle diseases like Malignant Hyperthermia (MH) or Central Core Disease (CCD) and multi-minicore disease (MmM). MH is a potentially lethal pharmacogenetic disorder of skeletal muscle, inherited in an autosomal dominant mode. The incidence of MH episodes during anesthesia is between 1:5,000 and 1:50,000–100,000 anesthesias whereas the estimated prevalence of the genetic abnormalities may be as high as 1:3000 individuals (range 1:3,000 to 1:8,500)[20]. MH clinical episodes are triggered in susceptible individuals by exposure to volatile anesthetics (halothane) or depolarizing muscle relaxants. An MH crisis is characterized by increased muscle metabolism and heat production resulting in a progressive hyperthermia and muscle rigidity associated with tachycardia, metabolic acidosis, hyperkalemia and hypoxia. Apart from induced crisis episodes, MH patients do not present clinically relevant symptoms. Because of its subclinical nature, MH susceptibility has to be usually diagnosed by an invasive *in vitro* contracture test (IVCT). According to the European standardized protocol[21], the contracture responses of muscle tissue upon the exposure to halothane and caffeine discriminate individuals as MH susceptible (MHS), MH normal (MHN) and MH equivocal (MHE). The last category encompasses patients who react abnormally to one but not both of the triggering agents used. Unfortunately, so far the diagnosis of MH susceptibility cannot be made using a simple genetic test because the high level of genetic heterogeneity does not avoid the risk of false MH-negative diagnoses. However, there may be situations where genetic data provide additional

diagnostic information or contribute information independent of IVCT, according to the recently diagnostic guidelines from the European MH Group [22].

All the symptoms of the MH crisis demonstrate the relevant consequences of altered EC coupling that results in an abnormal and uncontrolled Ca^{2+} release from SR stores within skeletal muscle following the administration of anesthetics and muscle relaxants.

Genetic heterogeneity of MH

Malignant hyperthermia displays a high level of *locus* heterogeneity. The first molecular genetic studies had shown that the human MHS trait maps to the ryanodine receptor *locus* (RYR1 gene) on chromosome 19q13.1 [23, 24]. The RYR1gene encodes the skeletal muscle Ca^{2+} release channel of the SR. Linkage studies established RYR1 as the main MH causing gene that accounts for susceptibility in more than 50% of MH families. So far, more than 150 mutations, clustered in structurally and functionally definable areas in RyR1, have been identified in MHS families [25] but only 28 of them have been functionally validated (www.emhg.org) and can be used for molecular diagnosis. With the exclusion of linkage between MHS and RYR1 on several occasions [26], it has become apparent that the genetic basis of MH is very complex. As MH is thought to be induced primarily by abnormalities in skeletal muscle Ca^{2+} homeostasis, the five protein-subunits of DHPR encoded by four separate genes have been considered as plausible candidate genes for MHS. So far, from this entire complex, only the CACNA1S gene encoding the DHPR-α_{1S} subunit on chromosome 1q32 [27, 28] (MHS5, MIM 601887) and the gene encoding the DHPR-$\alpha_2\delta$ subunit on chromosome 7q21-22 [29] (MHS3, MIM 154276) showed association to MH susceptibility. A genome wide search has identified 3 additional MHS *loci*. One of these locates on chromosome 17q11-24 [30] (MHS2, MIM 154275), the site of the SCN4A gene encoding the α subunit of the sodium channel. The other two *loci* are on chromosome 3q13.1 [31] (MHS4, MIM 600467) and 5p [32] (MHS6, MIM 601888), where no candidate genes have been identified so far.

Aim of this thesis

This Ph.D. thesis presents the functional characterization of a new MH point mutation, T1354S, identified in the CACNA1S gene [28]**.** As described in my degree thesis, we found co-segregation of markers close to the CACNA1S gene in all MHS individuals of a south Italian family. LOD-score values between these markers and the disease were equal or close to 1.76, the maximal expected value for this pedigree. DNA sequence analysis of the CACNA1S gene of MHS members of the family revealed the presence of an A4062T transversion in exon 33 at the heterozygous status resulting in the substitution of threonin 1354 for serine (T1354S). The substituted amino acid residue is located in the IVS5-S6 extracellular P-loop of α_{1S}. Mutation T1354S was detected neither in related MH normal individuals nor in 134 unrelated control subjects. Here I present investigations of the effects of the T1354S mutation on the assembly and function of the EC-coupling apparatus after transiently expressing the mutant α_{1S} T1354S in dysgenic (α_{1S} null) murine myotubes.

MATERIALS AND METHODS

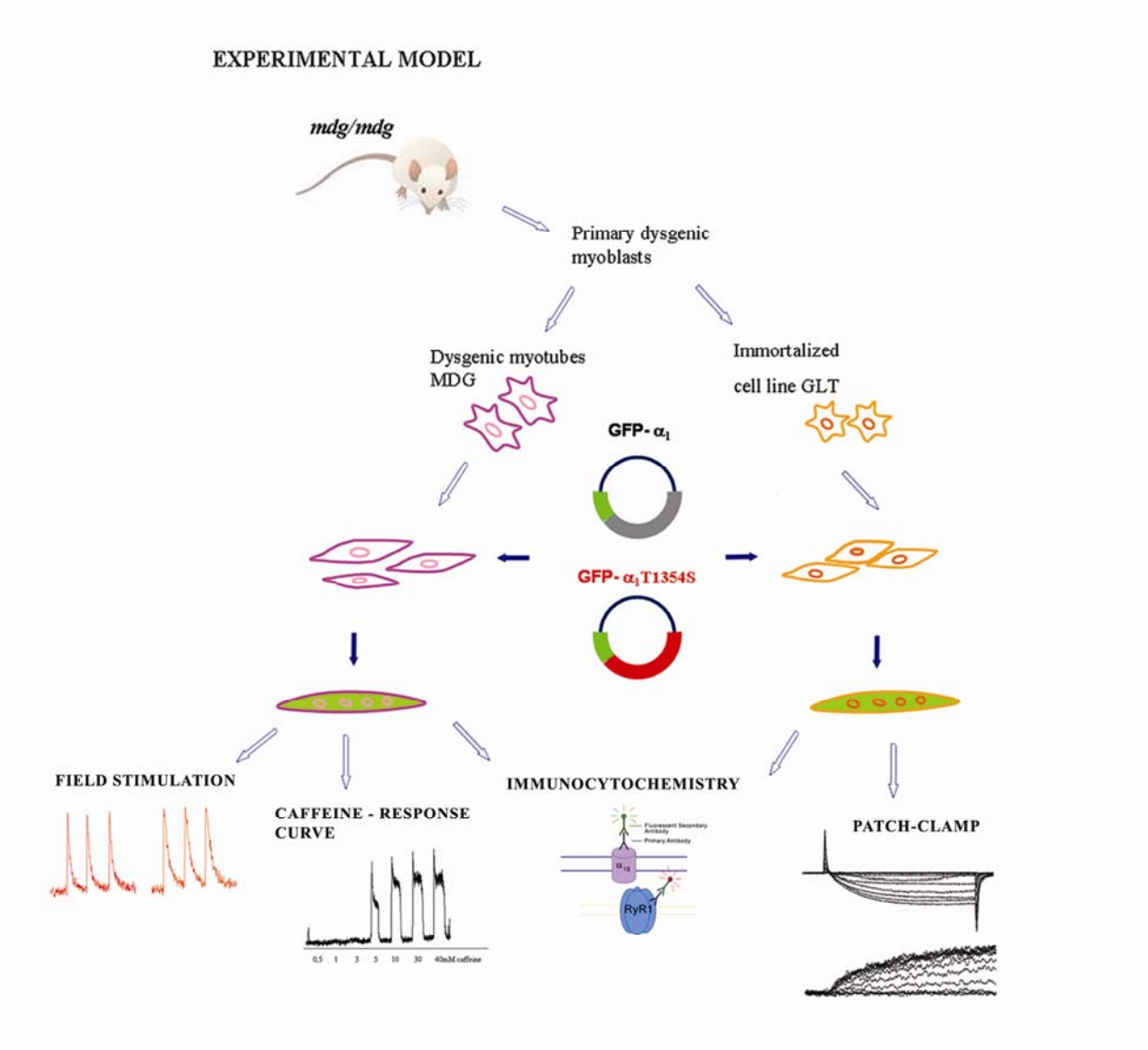

- **Dysgenic myotubes**
- **Immunocytochemistry**
- **Patch-clamp**
- **Caffeine response curve**
- **Field stimulation**

Dysgenic Myotubes

All the experiments were performed in dysgenic (α_{1S} - null) myotubes, explicitly GLT and MDG.

- The skeletal muscle cell line GLT derived from dysgenic-mouse skeletal muscle cells [33], transfected with a plasmid encoding a Large T antigen [34]. GLTs muscle cells are flatter than the primary cultures and they need to be adherent to the substrate to grow and differentiate. These cells lack the α_{1S} subunit of DHPR while the $\alpha_2\delta$ is present but not correctly targeted. Nevertheless, RyRs are normally expressed and clustered in correspondence of the T-tubule/SR junctions, thus we can observe in GLTs only Ca^{2+} release induced by caffeine but not spontaneous or depolarization-induced Ca^{2+} release from SR.
  Mononucleated GLT cells are continuously cultured in growth medium (GM).

  ***Growth Medium**:*

  - *80% DMEM*
  - *10% fetal calf serum (FCS)*
  - *10% horse serum (HS)*
  - *2mM L-glutamine*
  - *100U/ml penicillin/streptomycin*

  GLTs are plated every two days (70% confluent) on 35 mm culture dishes or on glass cover slips and cultured on GM for 2 days. When they reach approximately 80% confluence, GM is changed to fusion medium (FM) to induce cell fusion and differentiation.

  Fusion Medium:

  - *98% DMEM*
  - *2% HS*
  - *2mM L-glutamine*
  - *100U/ml penicillin/streptomycin*

On day 4, cells are transfected with α_{1S} subunit cDNA. The liposome-mediated transfection (FuGENE, Roche) was found to be the best method for transfection of GLTs. After transfection, cells are cultured until day 7 on FM when they are very well differentiated with the α_{1S} subunit completely expressed. On days 7 and 8 these cells are used for experiments.

FuGENE transfection (according to the manufacturer`s instructions)

- *For each dish, mix 94 µl of DMEM with 6 µl of FuGene (pre-warmed at RT)*
- *Incubate for 5 min*
- *Provide 2 µg of DNA per dish in a transfection tube*
- *Add 100 µl DMEM/FuGene mix and incubate for 15 min*
- *Apply directly on the cells 100 µl of the transfection mix*
- *Incubate for 2 min and then add 1.5 ml of FM*

- MDG cells are dysgenic myotubes generated from primary myoblasts (from newborn dysgenic mice)[35, 36]. These cells are very similar to the primary cultures with earlier fusion and, like GLTs, they are continuously cultured on plating medium (PM), enriched with bFGF.

Plating Medium

- *80% F-10 Ham´s Media with L-Glutamine (200mM) and HEPES (25mM)*
- *20%FCS*
- *100U/ml penicillin/streptomycin*
- *βFGF (2.5-5ng /ml)*

MDG cells grow on collagen coated (5µg/cm^2) 10cm dishes (see protocol below) at 37ºC and 5% CO_2 until they reach 70-75% confluence. They are daily split 1:2 and plated on 35mm culture dishes or on glass cover slips coated with gelatin and cultured on GM for 1 day. On day 2, GM is changed with FM (same used for GLT cells) and on day 3 they are transfected with FuGENE, following the same protocol described for GLTs. The medium has to be changed

every day. They are cultured until day 9 for complete differentiation and used for the experiments.

Collagen coating of culture dishes

- ***Stock 1.*** *Mix collagen (solid) type I with 0.1M Acetic Acid, for a final concentration of 1mg/ml*
- ***Stock 2.*** *Mix* ***stock 1*** *solution with absolute ethanol and water in ratio of 1:1:2 (concentration of collagen = 0.25mg/ml)*
- *Coat each 10 cm culture dish (55cm^2) with 1.1ml of stock-2 (5µg/cm^2 collagen)*
- *Leave the dishes dry for 30 min*
- *Open the dishes and leave them air dry for other 40 min*
- *Wash two times the coated dishes with PBS 1X*
- *Let them perfectly dry.*

Construction of mutant α_{1S} T1354S

The wild-type (WT) clone GFP-α_{1S} was generated by fusing α_{1S}-subunit cDNA in-frame to the COOH terminus of the coding region of a modified green fluorescent protein (GFP) contained in a proprietary mammalian expression vector [37]. To construct the T1354S point mutation in GFP-α_{1S} [nucleotide numbers (nt) are given in parentheses and asterisks indicate restriction enzyme (RE) sites introduced by PCR with proofreading *Pfu* Turbo DNA polymerase], the silent *AccI** (nt 4056) and *SpeI** (nt 4526) RE sites together with a base substitution (nt 4066) that created a triplet coding for serine instead of threonine were introduced via the antisense primers by PCR. The *AatII-SpeI** fragment (nt 3596-4526) produced by this PCR step was coligated with the *XhoI/AatII* fragment of plasmid GFP-α_{1S} (nt 4328-5265) into the corresponding *XhoI-SpeI* RE sites of *pBluescript*. Subsequently, the *XhoI/BglII* fragment of this construct was inserted into the corresponding RE sites of GFP-α_{1S}. For simplicity, we refer to this construct as α_{1S}T1354S. All sequences generated and modified by PCR were checked for integrity by sequence analysis (MWG Biotech, Ebersberg, Germany).

Other α_{1S} constructs

Beside the α_{1S}WT [35] and the mutant α_{1S}T1354S, other α_{1S} constructs were used as controls: a high conductive channel (α_{1S} hc) and no-conductive channel (α_{1S} nc).

α_{1S} hc is a new splice variant of α_{1S}, characterized by very high and fast L-type calcium currents. These data are not yet published.

α_{1S} nc is a mutant α_{1S} with a single point mutation D396K. This construct was generated by the substitution in the rabbit α_{1S} of an Aspartic acid with Lysine, which is normally present in the medaka α_{1S}.

Immunocytochemistry

Immunocytochemistry allowed us to verify the expression of the transfected α_{1S} subunits, the correct colocalization of the two Ca^{2+} channels, DHPR and RyR1, in correspondence of the T-tubule/SR junctions and the correct targeting of $\alpha_2\delta$ in the plasma membrane. For double labeling (Fig. 5), we used a combination of primary antibodies (anti-α_{1S} or anti-GFP, anti-RyR1 and anti-$\alpha_2\delta$) and fluorescent secondary antibodies (Tab.1).

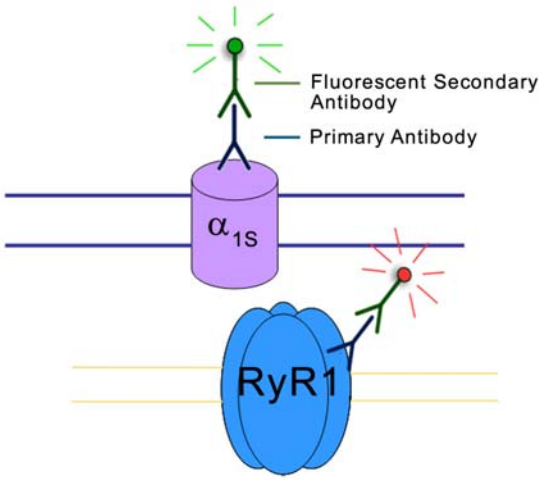

Fig. 5. Double immunostaining. Primary antibodies, raised in rabbit or mouse, and fluorescent secondary (anti-rabbit, anti-mouse) antibodies are directly applied to fixed myotubes. Secondary antibodies are chosen such to give a wide separation of the fluorescence signals.

According to the protocol described below, differentiated myotubes were fixed, the plasma membranes were permeabilized and the primary antibodies raised in rabbit or in mouse, were directly applied. In the next step, secondary antibodies, labeled with Alexa-488 or Alexa-598 to achieve a wide separation of the fluorescence signals, were applied. Alexa-488 was usually used with the anti-GFP antibodies so that the antibody label and the intrinsic GFP signal were both recorded in the green channel.

Images were recorded on a Zeiss Axiophot microscope with a cooled charge-coupled device (CCD) camera and MetaView image-processing software (Universal Imaging, West Chester, PA). The screening of coverslips of transfected myotubes with labeling pattern was performed systematically with a 63x objective.

Double immunofluorescence staining protocol

- *Rinse cells with phosphate-buffered saline (PBS) at room temperature (RT)*
- *Fix cells in 100% methanol at -20ºC for 10min*
- *Rehydrate by plunging the coverslips with the adherent cells into PBS*
- *Incubate the cells for 30 min with 5% normal goat serum in PBS containing 0.2% BSA and 0.2% Triton X-100*
- *Incubate with primary antibodies prepared in PBS/BSA/Triton (Tab. 1 for the dilutions used) for 2 hours at RT or overnight at 4ºC*
- *Wash in five changes of PBS/BSA/Triton*
- *Incubate with fluorescent secondary antibodies (Tab.1) in dark for 1hour*
- *Wash again in five changes of PBS/BSA/Triton*
- *Mount in PPD-Glycerol (90% Glycerol, 0.1M Tris/HCl, pH=8, 5mg/ml p-phenylen diamin) to impede photobleaching.*

Tab.1

Primary Ab	***Specificity***	***dilution***	***Secondary Ab (1:4000)***
Monoclonal, m1A	α_{1S}	*1:2000*	*Goat-anti mouse A-488*
Affinity purified, rbGFP	*GFP*	*1:5000*	*Goat-anti rabbit A-488*
Monoclonal, m20A	$\alpha_2\delta$	*1:1000*	*Goat-anti mouse A-594*
Affinity purified, rbRyR-162	RyR1	*1:2000*	*Goat-anti rabbit A-488* *Goat-anti rabbit A-594*

Whole-cell patch clamp

Patch clamp is a technique that allows the study of ion channels in excitable cells. There are different variants of this technique, according to the aim of the researcher. In our case, to study the electrical behavior of all ion channels in the entire cell-membrane, we used the *whole-cell recording method* (Fig. 6). A glass pipette with a very small tip is used to make a tight contact with a tiny area (or patch) of cell membrane thereby showing electrical resistance in the giga Ohm range (so-called "gigaseal") Applying a strong suction, the membrane patch within the pipette mouth is disrupted and the solution inside the pipette (resembling the intracellular environment) becomes continuous with the cytoplasm of the cell. In this configuration, the membrane potential of a cell is clamped at a constant value (*voltage clamp technique*, Fig. 7) and the current that flows through the membrane at any particular potential can then be measured. The principle of this technique is to inject a current which is equal in amplitude but opposite in sign to the current flowing across the cell. This results in no net current flow across the membrane, and the membrane potential remains constant. Therefore, by measuring the current, which has to be injected to clamp the potential, the current flowing across the membrane can be determined. By measuring currents at different clamped membrane potentials it is then possible to characterize voltage-gated ion channels.

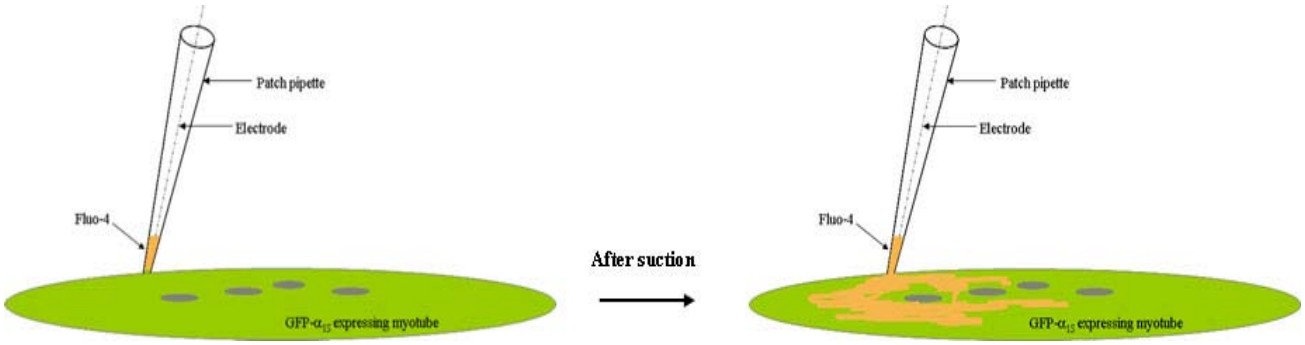

Fig. 6. Patch-clamp. A freshly pulled glass pipette with a tip diameter of few micrometers is pressed gently on the cell membrane to form a "gigaseal" (pipette resistance in giga Ohm range). When suction is applied to this patch pipette the membrane breaks under the pipette (open conformation) and the pipette solution diffuses into the cytoplasm. In this conformation and with a specific ion composition of the pipette solution and specific pulse protocols, it is possible to measure ion currents across the whole membrane of one cell.

The Ca^{2+} currents were monitored in GLT myotubes on days 7 or 8, cultured in 35 mm culture dishes and mounted on an Olympus IX70 inverted microscope equipped with Hoffmann modulation contrast. All recordings were performed with an Axopatch 200A amplifier controlled by pClamp 7.0 software. Myotubes were bathed in an external solution that contained 145mM tetraethylammonium (TEA)-Cl, 10mM $CaCl_2$ and 10mM HEPES (pH 7.4 with TEA-OH). Patch pipettes were pulled from borosilicate glass (Harvard Apparatus), fire-polished (Microforge MF-830, Narishige), and had resistances of 1.5–2.5 MΩ when filled with a solution consisting of 145mM Cs-aspartate, 2mM $MgCl_2$, 10mM HEPES, 0.1mM Cs-EGTA, 2mM Mg-ATP (pH 7.4 with CsOH). For simultaneous recordings of L-type currents and intracellular Ca^{2+} transients, the pipette solution additionally contained 0.2mM fluo-4 pentapotassium salt. Depolarization-induced intracellular Ca^{2+} transients were monitored from a small rectangular region of the myotube with a photomultiplier detection system (Photon Technology International, South Brunswick, NJ).

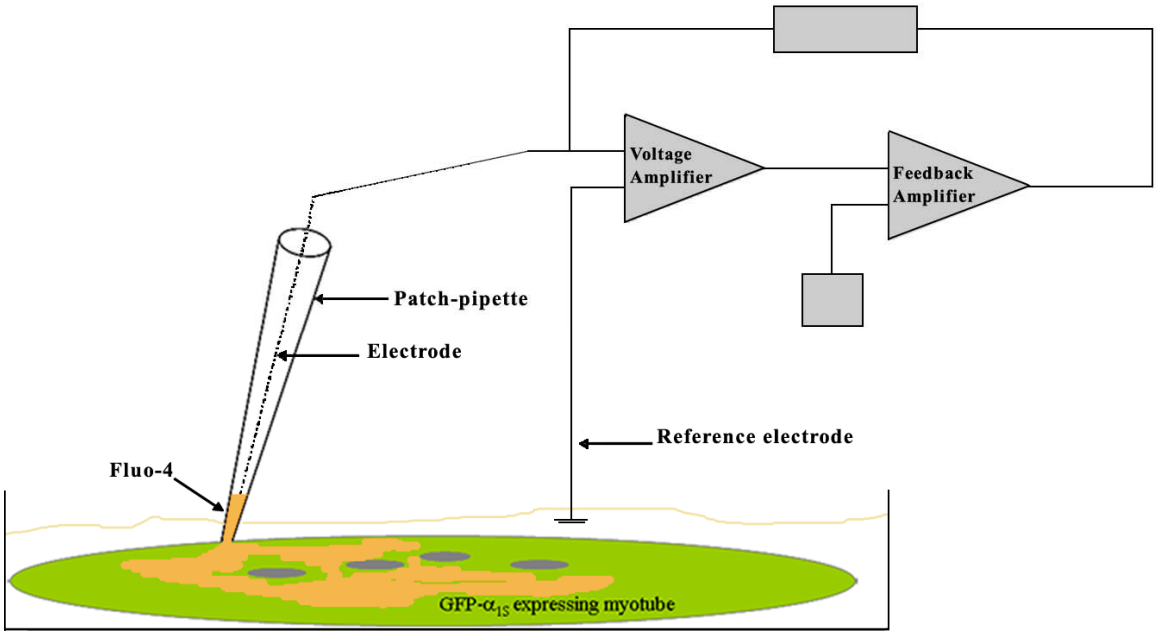

Fig. 7. Voltage clamp patch clamp. Voltage clamp is based on a feedback system where a measured membrane potential is constantly compared and subtracted from a command voltage (CV), selected by the experimenter. Any difference is instantaneously compensated by current that is an accurate estimation of the ionic currents of the entire cell membrane.

In some experiments, voltage-gated Ca^{2+} release was also monitored in the presence of a low concentration (2mM) of extracellular caffeine. According to a standardized protocol, L-type currents were elicited with 200-ms depolarizing steps from a holding potential of –80 mV to test potentials between –50 and +80 mV in 10-mV increments.

In all recordings, linear leak and capacitative currents were digitally subtracted with a P/4 prepulse protocol. To inactivate low voltage-activated T-type currents, each test pulse was preceded by a 1-s prepulse to –30 mV. Recordings were low-pass Bessel filtered at 2 kHz and sampled at 5 kHz. Ca^{2+} currents were normalized by linear cell capacitance (expressed in pA/pF). The L-channel conductance (G) for each test voltage (V) was obtained with the following equation:

$$G(V) = -I_{Ca} / (V - V_{rev})$$

where I_{Ca} is the peak Ca^{2+} current during the test pulse, V_{rev} is the extrapolated reversal potential, and V is the membrane potential.

The voltage dependence of L-type currents (Q) and intracellular Ca^{2+} release (ΔF/F) was fitted according to a Boltzmann distribution:

$$Y = Y_{max} /\{ 1 + \exp [- (V-V_{1/2})/ K] \}$$

where Y is Q or ΔF/F; Y_{max} is Q_{max} or $(\Delta F/F)_{max}$; $V_{1/2}$ is the potential at which $Y = Y_{max}/2$; and k is a slope factor.

The activation phase of Ca^{2+} current (0 to current level to 98% of peak current amplitude) was fitted with the following single and double-exponential functions:

$$I (t) = A_{mono} * [\exp (-t/\tau_{mono})] + C$$

$$I (t) = A_{fast} * [\exp (-t/\tau_{fast})] + A_{slow} * [\exp (-t/\tau_{slow})] + C$$

where I(t) is the current at time t after depolarization, A_{mono}, A_{fast}, A_{slow} are the steady state current amplitudes of each component with their respective time constants of activation (τ_{mono}, τ_{fast}, τ_{slow}), and C represents the steady state peak current.

All recordings were made at room temperature (~27°C) and data are reported as means ± SE. Only currents with a maximal voltage error <5 mV due to series resistance were analyzed with Clampfit 8.0 (Axon Instruments, Foster City, CA) and SigmaPlot 8.0 (SPSS) software.

Measurements of caffeine induced Ca^{2+} release in myotubes

Increased sensitivity to activation by caffeine (0.5, 1, 1.5, 2, 3, 4mmol/l) is a primary diagnostic tool for MH susceptibility. Here we tested whether the MH mutation T1354S also increased the caffeine sensitivity of Ca^{2+} release via RyR1. In these experiments, we applied different caffeine concentrations (0.5 to 40mM) on MDG myotubes, cultured on big glass cover slips. Because caffeine quenches the fluorescence of single-wavelength Ca^{2+} dyes (e.g., fluo-4), the detection of Ca^{2+} release at threshold concentrations might be obscured. For this reason, we performed the caffeine curves with Indo-1, a ratiometric Ca^{2+} indicator that exhibits a Ca^{2+}-dependent shift in its emission wavelengths. Indo-1 requires a single excitation wavelength at 350nm and changes the emission spectra on binding Ca^{2+} from ~485 in Ca^{2+}-free

medium to ~405 nm when the dye is saturated with Ca^{2+}. Caffeine applications produce a comparable quench of both emission wavelengths and thus there is no effect on the resulting Indo-1 ratio (405/485) [38]. First of all, the sensitivity of the photomultipliers to acquire Indo-1 fluorescence was tested. A photomultiplier consists in a photocathode, several dynodes (in our case 9) and anode. When a photon of sufficient energy strikes the photocathode, it emits electrons due to the photoelectric effect. These few electrons are accelerated towards a series of additional electrodes called dynodes. Each dynode is placed at more positive potential then the previous one, so additional electrodes ca be generated at each dynode. This amplified signal is finally collected at the anode where it can be measured. The amplification of electrons depends on the number of dynodes and on the accelerating voltage. The voltage has to be selected in the way that the amplified signal could reach always the saturation. To this aim, the fluorescence of cells before and after Indo-1 loading was measured applying different test voltages to the photomultipliers. The amplified signal reached saturation when voltages higher than 800V were applied to both the photomultipliers (Fig. 14A). No difference was observed between untransfected and GFP-transfected cells (Fig. 14B).

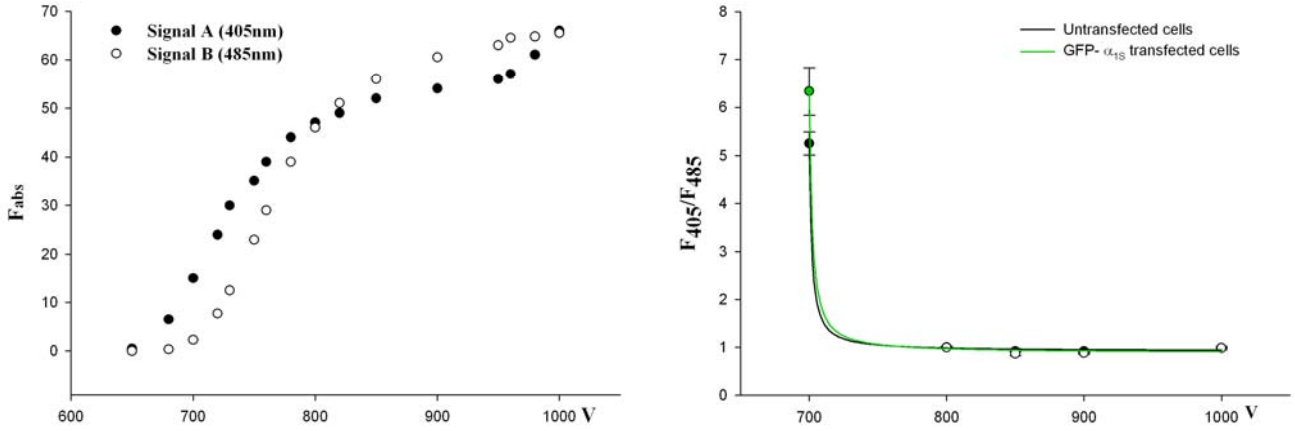

Fig. 14. Test of the photomultiplier sensitivity. To acquire maximal fluorescence signals, both photomultipliers (for both the emission wavelengths) require voltage higher than 800V(A). This test was made in untransfected and GFP transfected cells (B).

Next question was to estimate the contribution of the cell autofluorescence and the background fluorescence, on the total signal. To this aim, the fluorescence of a small area with and without

cell was measured. Before loading the cells with Indo-1, the cell-autofluorescence represented the 25% and 20% of the background fluorescence signal, respectively at 405 and 485nm (Fig.15). After Indo-1 loading, the background fluorescence component was approximately 25% and 15% of the total fluorescence signals at 405 and 485nm, respectively, whereas the cell-autofluorescence was approximately not higher than 5% of the total fluorescence signal (Fig. 15B). On the basis of these results, at the beginning of each recording, the background fluorescence, was measured in a cell-free area (corresponding exactly to the area with the selected cell) and automatically subtracted from the fluorescence signal, acquired during caffeine dose response recording.

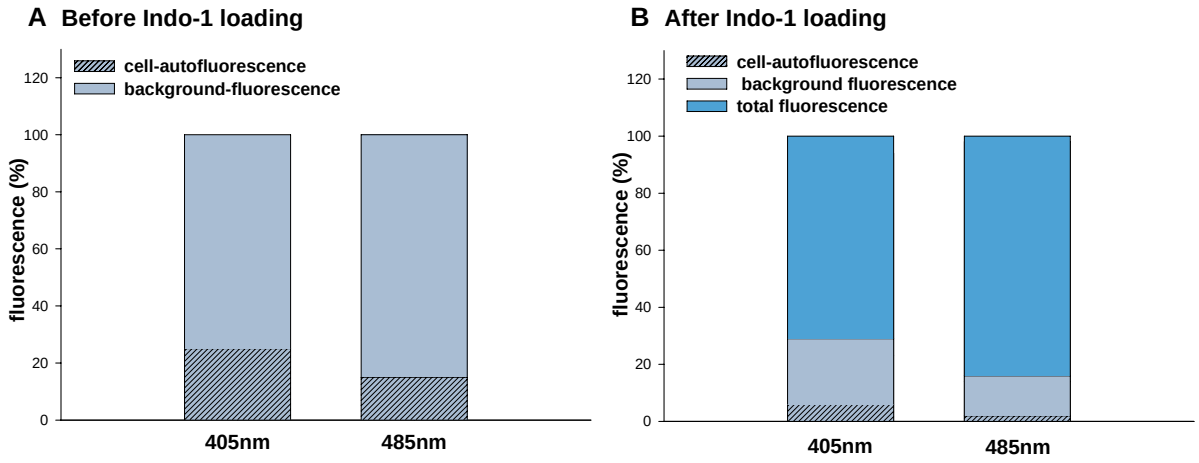

Fig. 15. Components of fluorescence. The cell-autofluorescence contributes approximately for 20% to the background fluorescence before loading the cells with Indo-1 (A). After loading, the background fluorescence is approximately 20% of the total fluorescence signal whereas the cell-autofluorescence is approximately 5% (B).

Myotubes were incubated for 1h at RT with 6μM Indo-1 plus 0.12% Pluronic in 1ml DMEM colorless. When loaded, myotubes were bathed in a normal rodent Ringer solution [containing 145mM NaCl, 5mM KCl, 2mM $CaCl_2$, 1mM $MgCl_2$, and 10mM HEPES, pH 7.4] and excited at 350 nm with a DeltaRam illumination system (Photon Technology, Princeton, NJ). Fluorescence emissions at 405 (F_{405}) and 485 (F_{485}) nm were collected with a photomultiplier detection system, and results presented as ratio (R) of F_{405} to F_{485}. Before each recording a small area of a single myotube was selected in the photomultiplier detection window. From a

window of the same size like the selected myotube region, background fluorescence was taken from a cell-free region of the glass cover slip and was automatically subtracted. At the beginning of each experiment, each responding cell, identified by its fluorescent signal (blinking), was electrically stimulated three times (10V for 2ms at 0.3 Hz) with two stimulating electrodes. The myotubes were then sequentially exposed to 60-s applications of different concentrations of caffeine (0.5, 0.7, 1.0, 3.0, 5.0, 10, 30 and 40mM), prepared in Ringer solution. Caffeine was directly applied to individual myotubes with a rapid perfusion system (Warner Instrument, Hamden, CT) that permits fast, local application of the agonist as well as rapid washout with control solution. Each caffeine application step was followed by a 60-s wash with Ringer solution.

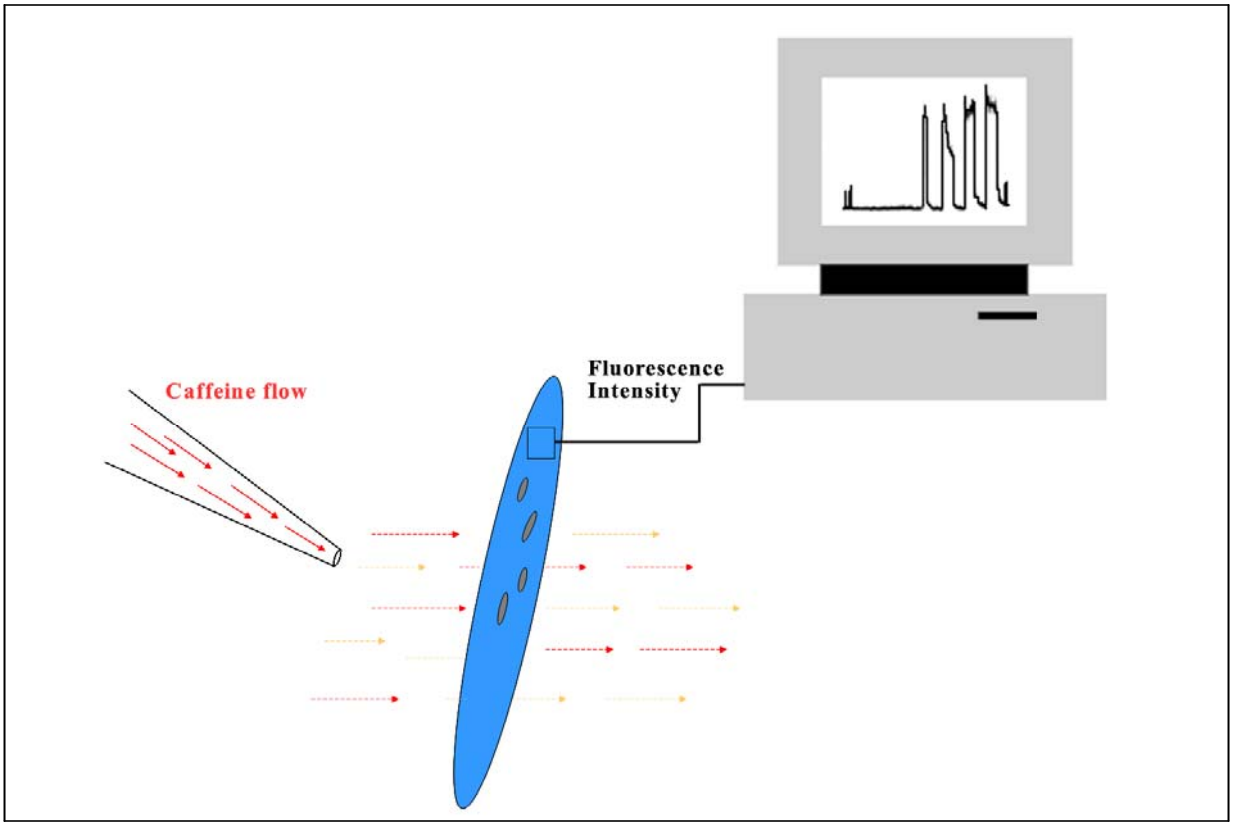

Fig. 7. Caffeine-induced Ca^{2+} release. Myotubes were loaded with Indo-1, a ratiometric Ca^{2+}-indicator, comprising a shift in emission wavelength upon binding Ca^{2+}. Each myotubes was perfused with different caffeine concentrations. The fluorescence emissions at 405nm and 485nm were collected in a photomultiplier detection system and displayed as ratios of F_{405} / F_{485}.

Peak intracellular Ca^{2+} changes in response to agonist application are expressed as ΔR ($R_{agonist} - R_{baseline}$). Data were analyzed with FeliX (Photon Technology, Princeton, NJ) and SigmaPlot 8.0 (SPSS, Chicago, IL) software packages. Caffeine concentration-response curves were fitted according to an equation of the following general form:

$$f(x) = D_{max}^{nH} / 1 + (EC_{50} / [D])^{nH}$$

where D_{max} is the maximal response, [D] is the caffeine concentration, n_H is the Hill coefficient, and EC_{50} is the concentration of caffeine at which the response is half-maximal.

Field stimulation

The Ca^{2+} release from intracellular store elicited by the action potential is a clear evidence for a normal EC-coupling mechanism. To verify this, myotubes previously loaded with fluorescent Ca^{2+} indicator Indo-1 are electrically stimulated in field stimulation experiments. The resulting change of Ca^{2+} levels is estimated via the changes in cellular fluorescence signals (visualised as "cell blinking").

Myotubes cultured on glass cover slips were incubated for 1h at RT with 6μM Indo-1. After incubation, the cover slip with cells was carefully washed and mounted on a specific chamber filled with Ringer solution on a Zeiss Axiovert epifluorescence microscopy. Transient elevations of intracellular Ca^{2+} were elicited by brief depolarizing pulses of 10V *2ms (at 0.3Hz, 5Hz *2s and 20Hz *2s) through a pair of electrodes, placed in two opposite side of the incubation chamber. Action potential Ca^{2+} transients were measured during a sequential exposition of the myotubes to 0, 1 and 2mM caffeine solution prepared in Ringer with 0, 2 or 10mM Ca^{2+}. The fluorescence signals were detected by a photomultiplier system (PTI 814) and analyzed by with FeliX and SigmaPlot 8.0.

RESULTS

The T1354S mutation does not affect α_{1S} targeting

Skeletal-type EC coupling depends on a protein-protein interaction between the sarcoplasmic Ca^{2+} release channel, RyR1, and the plasmalemmal voltage-gated Ca^{2+} channel, DHPR. This physical coupling requires a specific arrangement of four DHPRs in so called tetrads, positioned above every other RyR1 arranged in orthogonal arrays in the junctions of the plasma membrane or the plasmalemmal T-tubules with the SR [39].

First we wanted to know, if mutation T1354S might hamper proper DHPR membrane targeting. Myotubes of the dysgenic (α_{1S}-null) cell line GLT, transfected with GFP-α_{1S}WT and GFP-α_{1S}T1354S, were double labeled with an antibody against GFP, which is NH_2-terminally fused to each DHPR-α_{1S} subunits, as well as with an antibody against RyR1. Immunofluorescence analysis (Fig.8) showed that both, the transfected GFP-α_{1S}WT and the GFP-α_{1S}T1354S subunit are efficiently expressed in the dysgenic myotubes. The double labeling demonstrated that GFP-α_{1S}T1354S, exactly as GFP-α_{1S}WT, is organized in *clusters* that are perfectly colocalized with RyR1 *clusters*. This is particularly evident in the merged images (Fig.8C), in which the yellow foci represent the colocalization of GFP-α_{1S} subunit (green) and RyR1 (red).

The colocalization of the two channels is indicative of their location in junctions of the SR with the plasma membrane (peripheral couplings) or with the T-tubules (triadic couplings). DHPR-RyR1 coclustering was comparable in myotubes transfected with GFP-α_{1S} WT and GFP-α_{1S}T1354S. Thus, we concluded that the junctional targeting of DHPR is not affected by the MH point mutation T1354S, in the IVS5-S6 extracellular P-loop of α_{1S}.

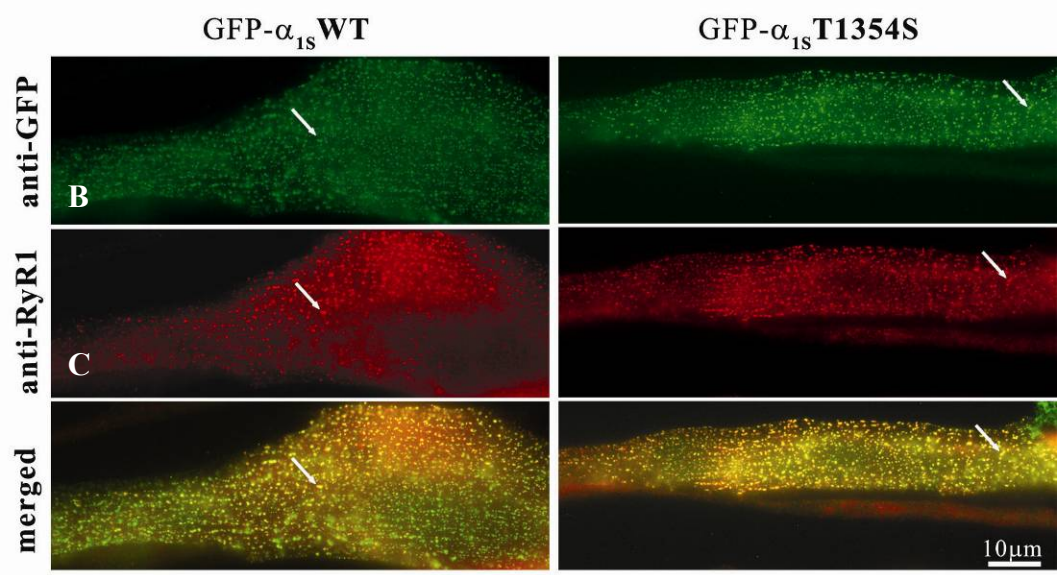

Fig. 8. DHPR-α_{1S} junctional targeting in skeletal muscle. Double immunofluorescence labeling was performed with antibodies anti-GFP and anti-RyR1, in dysgenic myotubes transfected with GFP-α_{1S}WT and GFP-α_{1S}T1354S. Both GFP-α_{1S} subunits are expressed and arranged in *clusters* (A: green) that colocalize perfectly with *clusters* of RyR1 (B: red), as shown in the merged image (C: yellow). This colocalization indicates correct targeting of DHPR and RyR1 in the junctions of SR and plasma membrane.

Current properties of α_{1S} T1354S

Skeletal-type EC coupling is known as a bidirectional signaling between DHPR and RyR1. In addition to the orthograde signaling, by which depolarization-induced conformational changes in the DHPR directly gate the opening of RyR1, also a retrograde signal exists, by which RyR1 controls the Ca^{2+} channel activity of DHPRs. Whole-cell patch clamp allows us to study the bidirectional DHPR-RyR1 signaling and to characterize the biophysical properties of the two Ca^{2+} channels. Whole cell patch clamp and intracellular Ca^{2+} measurements were performed to test whether the mutation T1354S could affect the function of DHPR as Ca^{2+} channel and as voltage sensor in EC coupling. Ca^{2+} currents in response to 200-ms depolarizing steps from a holding potential of –80 mV to test potentials between –50 and +80 mV in 10-mV increments were recorded in transfected myotubes, identified by the GFP fluorescence. Ca^{2+} currents and

depolarization-induced intracellular Ca^{2+} transients were measured simultaneously using the fluorescent Ca^{2+} indicator Fluo-4.

Representative recordings from dysgenic myotubes, transfected with GFP-α_{1S}WT and GFP-α_{1S} T1354S showed, that the expression of α_{1S}WT and α_{1S}T1354S restored L-type Ca^{2+} currents and Ca^{2+} transients (Fig. 9A-B). Comparable levels of Ca^{2+} influx in α_{1S}WT and α_{1S}T1354S expressing myotubes (Fig. 9B) indicated that the mutant channel was able to act as voltage sensor and Ca^{2+} conducting channel. At the same time, restored Ca^{2+} transients (Fig. 9A) indicated a functional interaction between DHPR and RyR1 channels. All the properties of Ca^{2+} currents are displayed in the Tab.2.

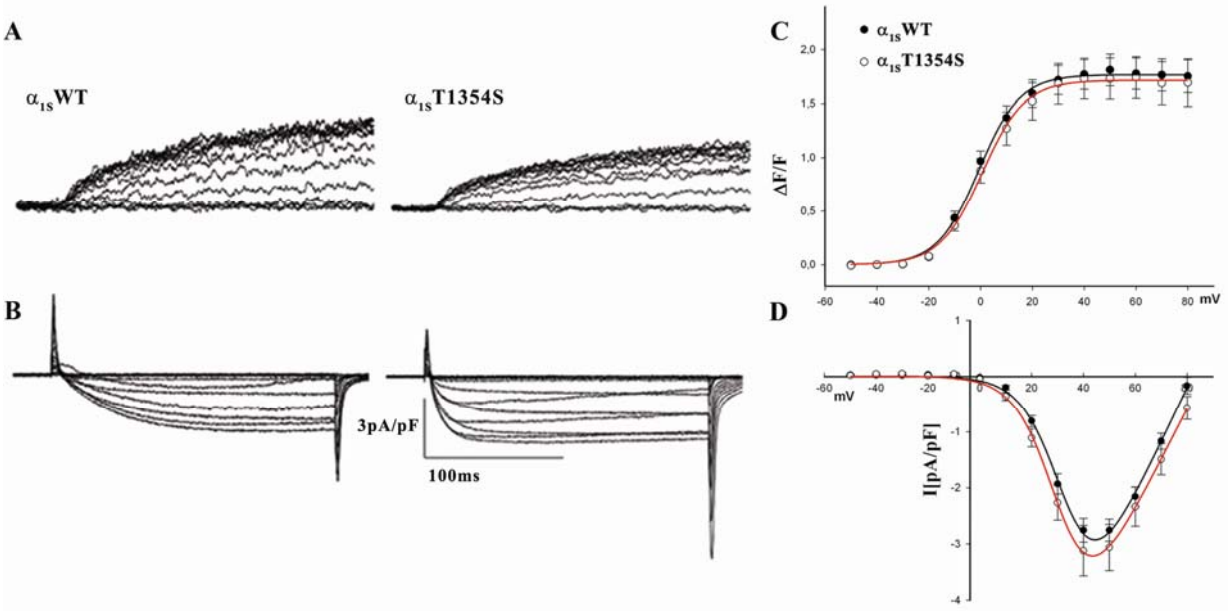

Fig. 9. Patch clamp recordings and intracellular Ca^{2+} measurements. Ca^{2+} release from the SR (A) and L-type Ca^{2+} currents (B) in response to 200ms depolarizing steps were recorded in α_{1S}WT and α_{1S}T1354S expressing myotubes. Voltage dependence and amplitudes of Ca^{2+} transients (C) and of Ca^{2+} currents (D).

The averaged amplitudes and voltage dependence of intracellular Ca^{2+} transients and Ca^{2+} currents were comparable in α_{1S}WT and α_{1S}T1354S expressing myotubes (Fig. 9C and D, Tab.2). Nevertheless, at first sight, a difference in the activation phase of L-type Ca^{2+} currents in the two channels appeared evident. In Fig. 9B, a representative recording from an α_{1S}WT transfected myotube shows slowly activating Ca^{2+} currents in contrast with the more accelerated traces recorded from α_{1S}T1354S transfected myotube.

Tab.2. Properties of Ca^{2+} transients and Ca^{2+} currents in α_{1S}WT and α_{1S}T1354S expressing myotubes, determined from intracellular Ca^{2+} fluorescence measurements and whole-cell patch clamp recordings. None of these values compared were significantly different.

		α_{1S}WT	α_{1S}T1354S
Ca^{2+} transients	**(ΔF/F)max**	**1.81 ± 0.14**	**1.74 ± 0.19**
	n	**40**	**27**
Ca^{2+} currents	**I_{max} (pA/pF)**	**2.97 ± 0.20**	**3.26 ± 0.44**
	G_{max} (nS/nF)	**103.6 ± 7.2**	**105.2 ± 11.2**
	V_{rev} (mV)	**80 ± 1.25**	**83 ± 1.76**
	n	**30**	**26**

As expected, the time to peak value (ttp), measured in correspondence of the maximal current traces (40mV or 50mV) was significantly (P<0.005) reduced from 99.87± 6.6 ms in WT (n=30) to 67.1±7 ms in the mutant channel (n=26) (Fig.10 A). Thus, the point mutation T1354S seems to play a role in the activation kinetic of skeletal muscle L-type Ca^{2+} currents. Similarly, the inactivation kinetic seems to be modulated by the T1354S mutation. The fractional inactivation (R_{200}) of the maximal current traces at the end of the 200-ms depolarization pulse was slightly, but not significantly (P=0.065), increased from 2.08±0.53 % in α_{1S}WT (n=30) to 4.12±1 % in α_{1S}T1354S (n=26) transfected myotubes (Fig.10 B).

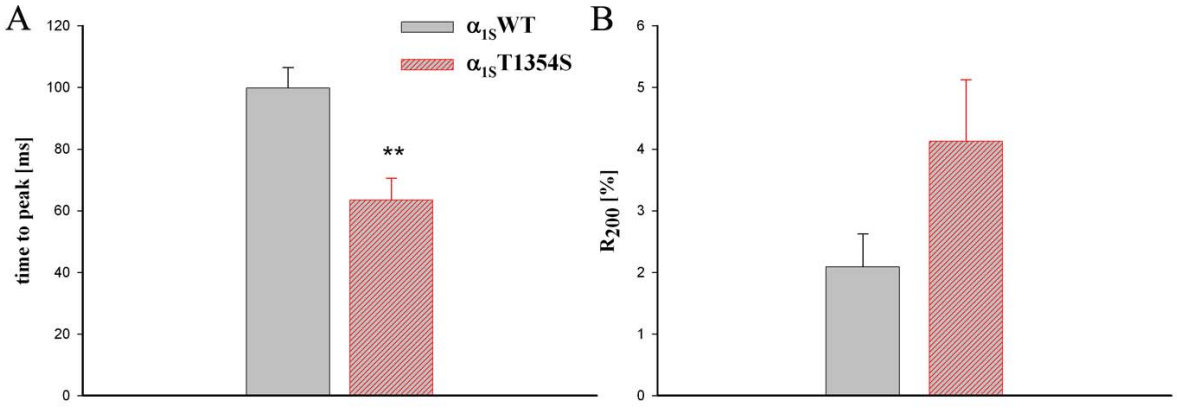

Fig. 10. Activation and inactivation analyses. Time to peak (ttp) of maximal Ca^{2+} currents is significantly (P<0.005) reduced in α_{1S}T1354S (A). The inactivation of Ca^{2+} currents at the end of a 200ms depolarization step, (R_{200}) is slightly (P=0.065) increased in α_{1S}T1354S-expressing myotubes (B).

Fast activation kinetics is an intrinsic property of α_{1S}T1354S

The DHPR Ca^{2+} channel is a multimeric complex where the main subunit, α_{1S} is responsible for voltage sensing and ion conduction, whereas the other subunits are involved in membrane targeting and modulation of current properties. In particular, $\alpha_2\delta$–1 is the determinant of the characteristic slow kinetics of skeletal muscle L-type Ca^{2+} currents. In normal skeletal muscle, the activation phase is described by two components of an exponential function characterized by their specific time constants (τ_{slow} and τ_{fast}). These components represent two populations of Ca^{2+} channel complexes: channels with $\alpha_2\delta$–1 and without $\alpha_2\delta$–1. In 2005, *Obermair et al.*[40] described that the depletion of $\alpha_2\delta$–1 results in accelerated activation kinetics and that the corresponding L-type Ca^{2+} currents are adequately fitted by a mono-exponential function with a single time constant (τ_{mono}), similar to the τ_{fast} in normal conditions. As the T1354S–α_{1S} mutation accelerates the activation kinetics of the Ca^{2+} channel and also under consideration of its localization on the extracellular IVS5-S6 loop, it could be possible that this mutation could disturb the interaction between α_{1S} and $\alpha_2\delta$–1. In order to clarify the mechanism of fast activated Ca^{2+} currents observed for the α_{1S}T1354S mutant channel, the maximal traces of L-type Ca^{2+} currents, recorded in α_{1S}WT and α_{1S}T1354S, were fitted with mono and bi-exponential functions. These analyses showed that in both channels (α_{1S}WT and α_{1S}T1354S) the fast and the slow components contribute equally to the total current amplitude (Fig.11A), even though the respective time constants (τ_{slow} and τ_{fast}) are significantly reduced ($P < 0.05$) in α_{1S}T1354S (Fig.11B). Similarly, a fraction of recordings, fitted adequately by a mono-exponential function, revealed for both constructs a single population of channels with a time constant (τ_{mono}) similar to the respective τ_{slow} (slow activating channels).

Taken together, these results reveal that the mutation T1354S does not disturb the balance between the fast and slow activating current populations and thus implicates an undisturbed interaction between the α_{1S} and $\alpha_2\delta$–1 subunits. However, the reduced time constant values (τ_{slow} and τ_{fast}),observed in α_{1S}T1354S, indicate that the mutation affects directly the activation kinetic properties of the α_{1S} subunit.

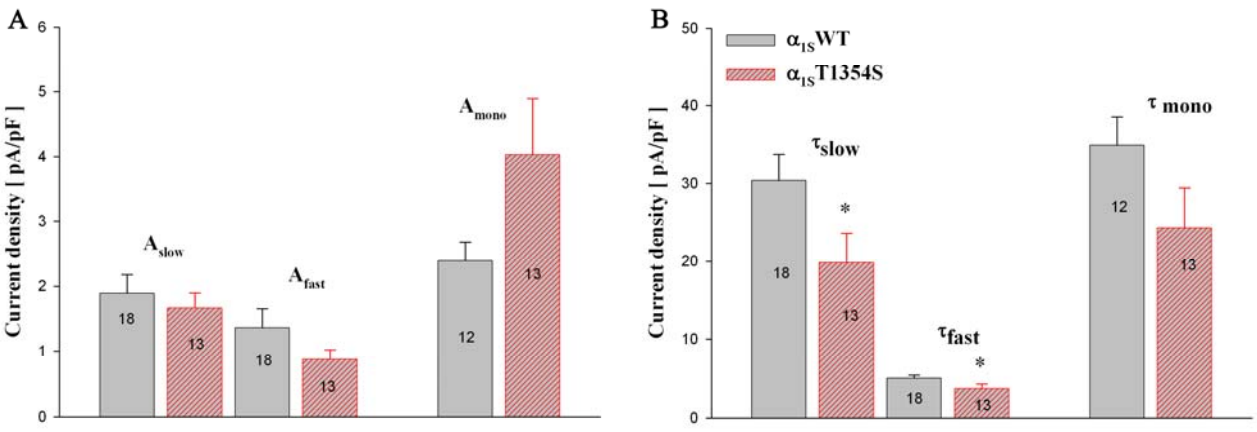

Fig. 11. Activation kinetics analysis. Kinetic analysis of Ca^{2+} currents shows the presence of both fast and slow components at similar ratios in α_{1S}WT and α_{1S}T1354S (A). However, the time constants of each component are reduced (* $p < 0.05$) for α_{1S}T1354S (B). Numbers of recordings are indicated inside the columns.

Tab 3. Parameters of Ca^{2+} current kinetics in α_{1S}WT and α_{1S}T1354S expressing myotubes. The Ca^{2+} currents were fitted with mono and bi-exponential equations. (* $p < 0.05$; ** $p < 0.005$)

Ca^{2+}currents		**α_{1S} WT (n)**		**α_{1S} T1354S (n)**	
	ttp **	**99.8 ± 6.6**	**(30)**	**67.1 ± 7.3**	**(26)**
	R_{200}	**2.08 ± 0.5**	**(30)**	**4.12 ± 1**	**(26)**
	τ_{slow}*	**30.4 ± 3.38**	**(18)**	**19.8 ± 3.7**	**(13)**
	τ_{fast}*	**5.05 ± 0.36**	**(18)**	**3.69 ± 0.5**	**(13)**
	τ_{mono}	**35 ± 3.6**	**(12)**	**24.3 ± 5.0**	**(13)**

The evidence for intact α_{1S} and $\alpha_2\delta$−1 subunit interaction as provided by this detailed kinetic analysis has also been supported by double-immunofluorescence labeling of GFP-α_{1S} and $\alpha_2\delta$−1 in dysgenic myotubes transfected with GFP-α_{1S}WT and GFP-α_{1S}T1354S. As previously published, $\alpha_2\delta$−1 subunits are diffusely expressed throughout the plasma membrane in dysgenic myotubes and it requires the expression of the α_{1S} subunit for its proper targeting into the triads[41]. Fig.12 shows that the T1354S-α_{1S} mutation does not alter the distribution of $\alpha_2\delta$−1 in clusters (Fig.12b) that are perfectly colocalized with clusters of α_{1S} (Fig.12a_1, c_1) indistinguishable from the situation in GFP-α_{1S}WT expressing myotubes (Fig. 12a, b, c).

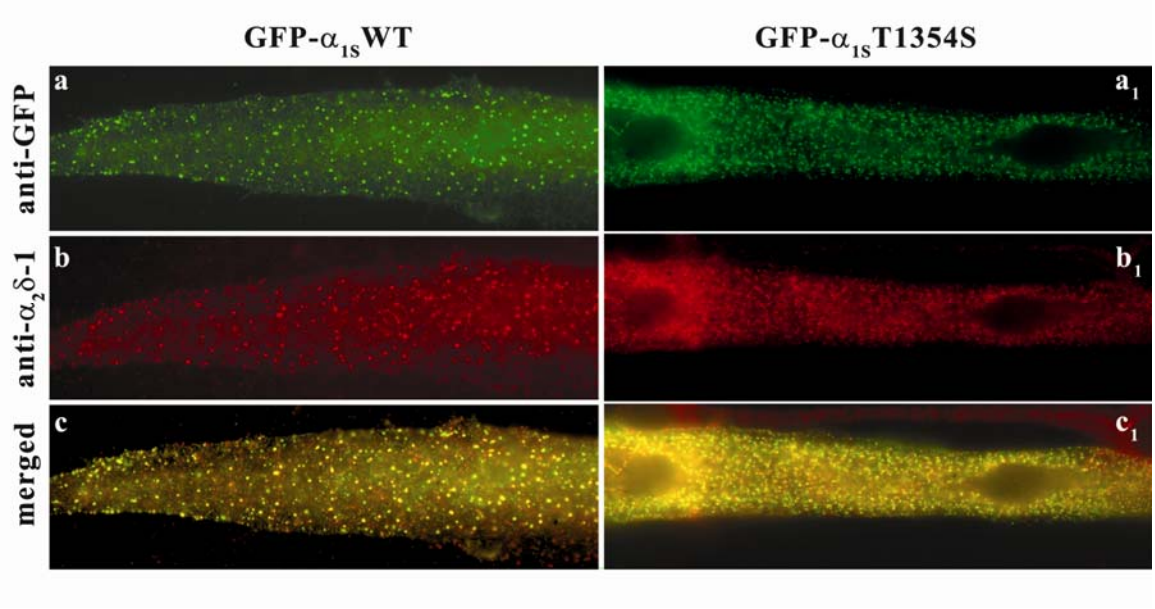

Fig. 12. **α_{1S} - $\alpha_2\delta$–1 colocalization.** Double immunofluorescence labeling was performed with antibody anti-GFP (a and a1) and anti-$\alpha_2\delta$–1 (b and b1), in dysgenic myotubes transfected with WT and mutant α_{1S} subunits. The $\alpha_2\delta$–1 subunits are arranged in clusters (b and b1) that colocalize perfectly with α_{1S} clusters (merged images c and c1).

Malignant Hyperthermia phenotype and enhanced caffeine sensitivity

The clinical manifestations of a malignant hyperthermia (MH) episode triggered by volatile anesthetics and depolarizing muscle relaxants are associated with a non-physiological increase of myoplasmic Ca^{2+} concentration. In addition, it is well known that skeletal muscle from MH susceptible (MHS) individuals show a higher response than muscles from MH normal (MHN) to RyR1 activators like caffeine and 4-chloro-m-cresol (4-CmC). This enhanced sensitivity is still used for the diagnosis of MH susceptibility by IVCT.

To test if the caffeine-induced Ca^{2+} release possibly contributes to a higher level of intracellular Ca^{2+} in presence of the T1354S α_{1S} mutation, Ca^{2+} currents and Ca^{2+} transients were patch-clamp recorded in α_{1S}WT and α_{1S}T1354S expressing myotubes after application of external solution containing 2mM caffeine. The averaged amplitudes and the voltage dependence of intracellular Ca^{2+} transients and of Ca^{2+} currents showed no differences between α_{1S}WT and α_{1S}T1354S expressing myotubes (Fig.13A). Nevertheless, the time to peak values

were found again significantly (P<0.02) reduced in α_{1S}T1354S (Fig.13B), thereby confirming the accelerated activation previously observed also under 2mM caffeine administration.

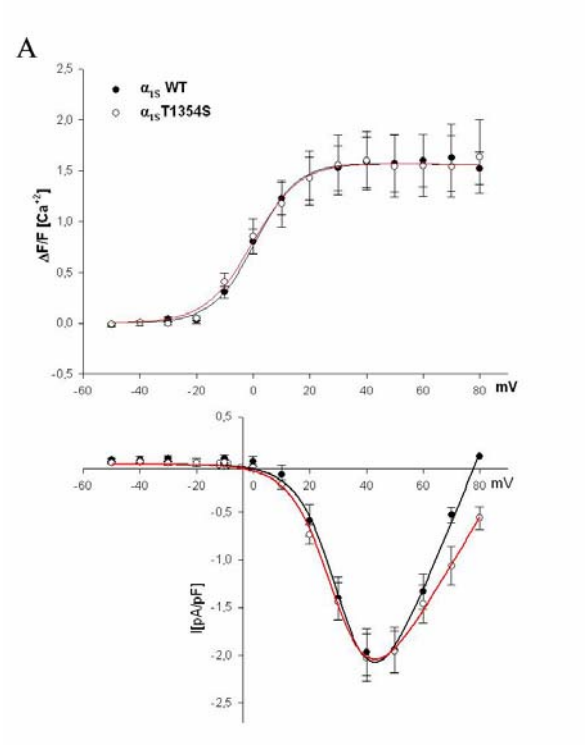

Fig. 13. Patch clamp recordings and intracellular Ca^{2+} measurements in external solution containing 2mM caffeine.
Amplitudes and voltage dependence of Ca^{2+}currents and Ca^{2+} transients, recorded in presence of 2mMcaffeine (A)

Time to peak (ttp) of Ca^{2+} currents were significantly (* P<0.02) reduced in α_{1S}T1354S (B)

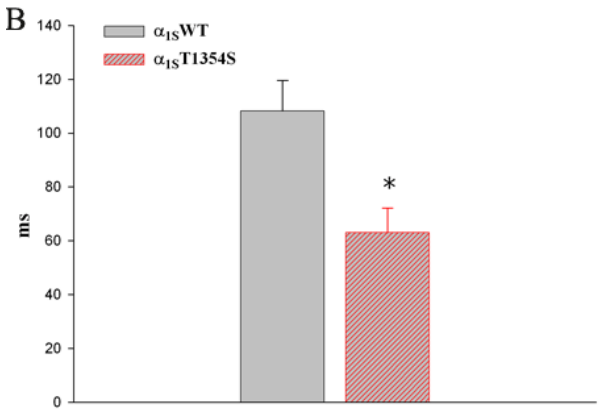

Enhanced caffeine sensitivity of RyR1 under control of α_{1S}T1354S ?

As already mentioned before, caffeine is an activator of RyR1 and is able to trigger Ca^{2+} mobilization from the SR. The activation of RyR1 induced by caffeine seems to be downregulated by the DHPRα_{1S} subunit[42] and is dependent on resting Ca^{2+} level[43], normally increased in the MH phenotype. According to these findings, it can be hypothesized that the T1354Sα_{1S}-mutation could account for an increased caffeine sensitivity of RyR1 by a hampered control function on the RyR1 activation. To this aim, caffeine dose response was assessed in α_{1S}-null, α_{1S}WT and α_{1S}T1354S-expressing GLT myotubes. Because caffeine quenches the single wavelength emission of Fluo-4 fluorescence, myotubes were loaded with

the ratiometric Ca^{2+} dye Indo-1. At the beginning of each caffeine dose-response recording, a rapid voltage-gated Ca^{2+} release was elicited by applying a train of three extracellular electrical stimuli (60V for 2ms) to confirm the functional expression of the DHPRs in transfected myotubes (Fig.16, see arrowheads). As expected, not any electrically evoked Ca^{2+} transient was observed in dysgenic GLT myotubes (left panel). Subsequently, the selected myotube was exposed to 60-s applications of caffeine with a stepwise increase from 0.3 to 40 mM, followed by a 60-s washout with Ringer solution (Fig.16).

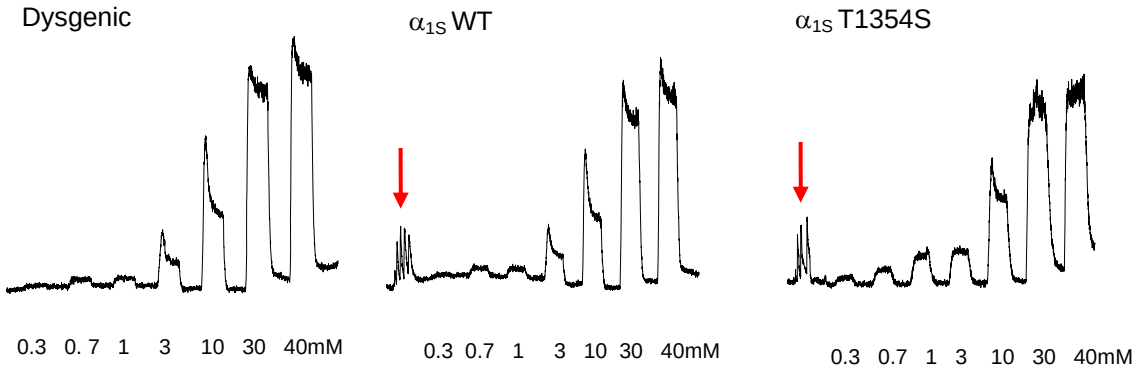

Fig. 16. Representative traces of caffeine concentration-response curves. Dysgenic untransfected and α_{1S}WT and α_{1S}T1354S transfected myotubes (GLT cell line) were loaded with Indo-1. At the beginning of each recording, electrical stimuli were applied to verify the expression of DHPRs. Increasing concentrations of caffeine (0.3 – 40 mM), separated by washing steps, were sequentially applied.

The caffeine response curve, in which each point represents the averaged maximal response to each caffeine concentration, showed that there was not a complete Ca^{2+} release even applying 40mM caffeine. As shown in Fig.17 (lines in black) dysgenic myotubes (cell line GLT), transfected or untransfected, seem to need higher caffeine concentrations to induce maximal release from SR. This finding is in contrast with previously published results[42] (Fig.17, red lines), where maximal Ca^{2+} release from SR was reported to be induced with 20 and 30mM caffeine.

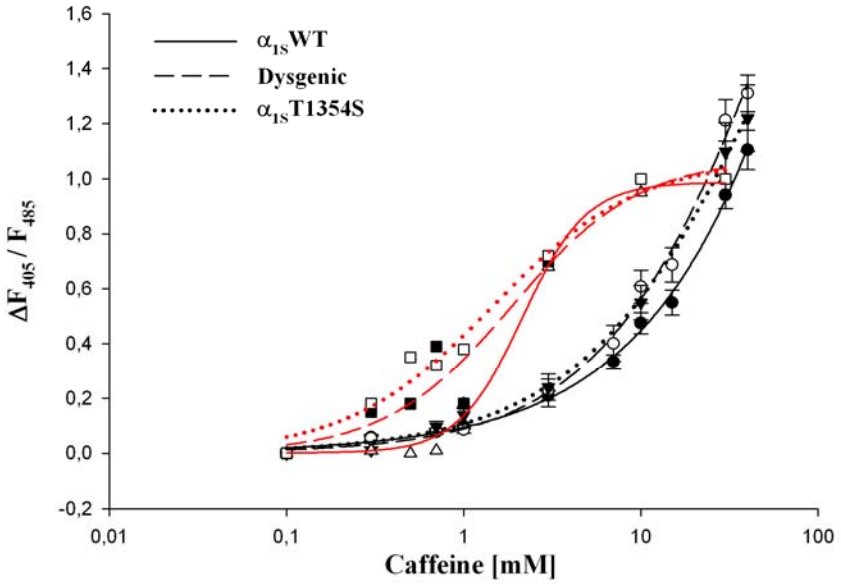

Fig. 17. Caffeine concentration-response curves comparing GLTs and published values.
The averaged values of maximal response, at the different caffeine concentrations are fitted according to the Hill equation. The caffeine dose response curves recorded in GLT myotubes (black lines) do not show saturation at highest (30-40mM) caffeine concentrations. In contrast, MDG cells (data taken from *Weiss at al.* 2004[42]) reacted with a maximal response to even lower caffeine concentrations (red lines).

To test whether this weak response was related to an intrinsic characteristic of the GLT cell line or to a wrong adjustment of the perfusion system, an immortalized cell line isolated directly from the transgenic Immortmouse, expressing the thermolabile SV40 large T antigen tsA58, was used (courtesy BE Flucher and G Kern)[44]. This cell line resembles much better the phenotype of primary mouse myotubes, and thus it was possible to verify that the weak caffeine response is only related to specific GLT cell line characteristics (Fig.18)

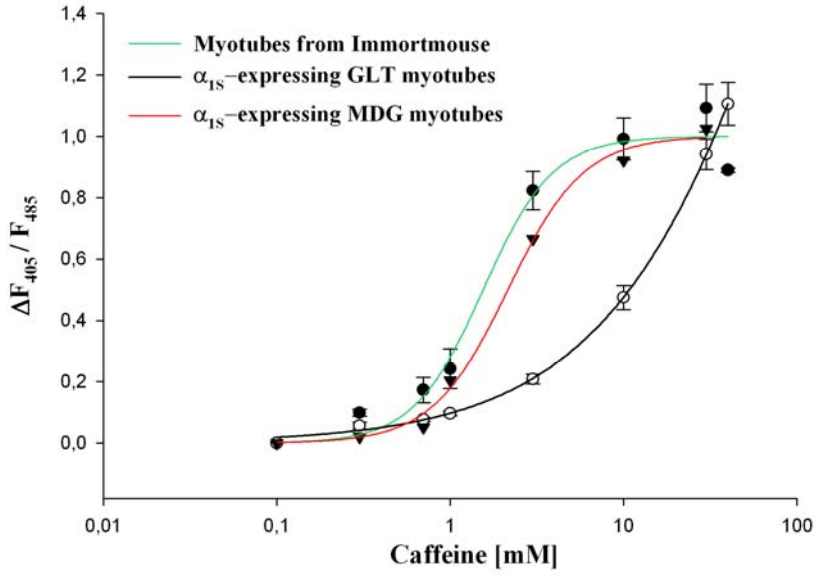

Fig. 18. Summary of caffeine concentration-response curves.
The response to caffeine is similar for MDG cells and immortalized myotubes in contrast to GLT myotubes that show weak caffeine-induced Ca^{2+} release and do not reach saturation even under high caffeine concentrations (40mM).

According to these findings, the dysgenic muscle cell line, defined as MDG cells [45] (courtesy of PD Allen and RT Dirksen) was used to proceed with the functional characterization of mutant α_{1S}T1354S.

Caffeine dose-response of α_{1S}T1354S expressed in MDG myotubes

Also for the MDG myotubes, liposome-mediated transfection (FuGENE and lipofectamine) was found to be the best method. As shown in Fig.19, patch clamp recordings and immunocytochemistry showed the correct expression of the transfected α_{1S}-subunits by restoration of Ca^{2+} currents, intracellular Ca^{2+} transients and proper membrane targeting.

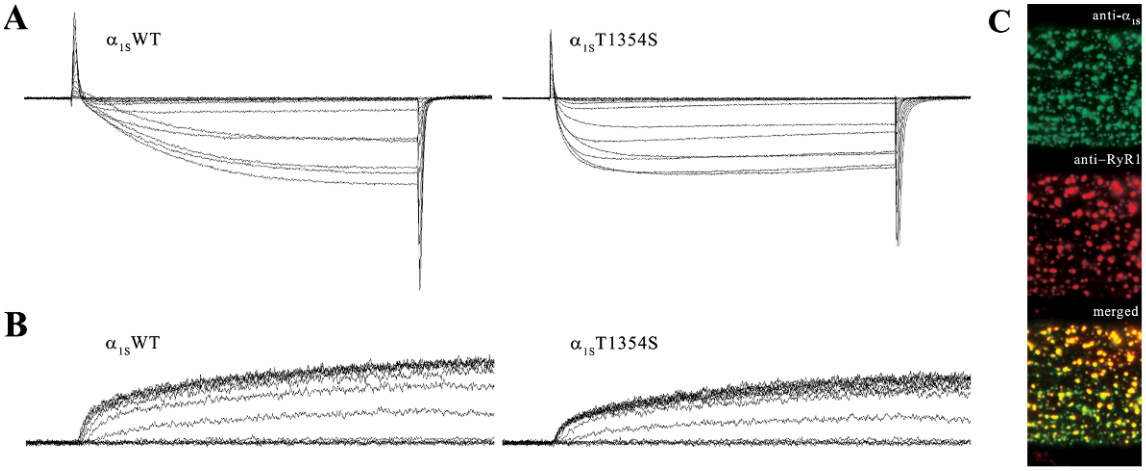

Fig. 19. Correct expression and targeting of transfected α_{1S} subunits in MDG myotubes. L-type Ca^{2+} currents (A) and intracellular Ca^{2+} transients (B) in response to 200-ms depolarization steps were restored after expression of GFP-α_{1S}WT and GFP-α_{1S}T1354S in MDG myotubes. Immunocytochemistry confirmed the perfect colocalization of α_{1S} subunits and RyR1 (C).

The caffeine dose-response experiments described above were repeated in MDG cells following the same protocol as used for GLTs.

Myotubes were loaded with the ratiometric Ca^{2+} dye, Indo-1 for 1 hour at 37°C. At the beginning of each recording, the selected DHPRα_{1S}-transfected myotube was electrically stimulated (10V*2ms) and the obtained voltage-gated Ca^{2+} release was judged as a

confirmation of the functional expression of the DHPR. Subsequently, the myotube was exposed for 60-s periods to increasing concentrations of caffeine (0.3-0.7-1-3-10-30-40mM), with each perfusion period separated by 60-s washes with Ringer solution. Caffeine concentration-response curves obtained from the averaged values of the maximal response to each caffeine concentration in untransfected MDG myotubes (n=19) as well as in α_{1S}WT (n=18) and α_{1S}T1354S (n=21) expressing myotubes were fitted according to the Hill equation. Even though maximal caffeine-induced Ca^{2+} release is similar in dysgenic, α_{1S}WT and α_{1S}T1354S-expressing myotubes, the caffeine-induced Ca^{2+} release curve is shifted to lower caffeine concentrations in untransfected dysgenic compared to α_{1S}WT-expressing myotubes. However, α_{1S}T1354S-expressing myotubes showed a sensitivity of caffeine-induced Ca^{2+} release intermediate between the dysgenic and WT values (Fig 20A). A similar graduation was also found if the data were analyzed by counting cells responding to lower (3 and 5 mM) caffeine concentrations. Responders were more frequently found in untransfected dysgenic myotubes, followed by α_{1S}T1354S-expressing and subsequently α_{1S}WT-expressing myotubes (Fig 20B).

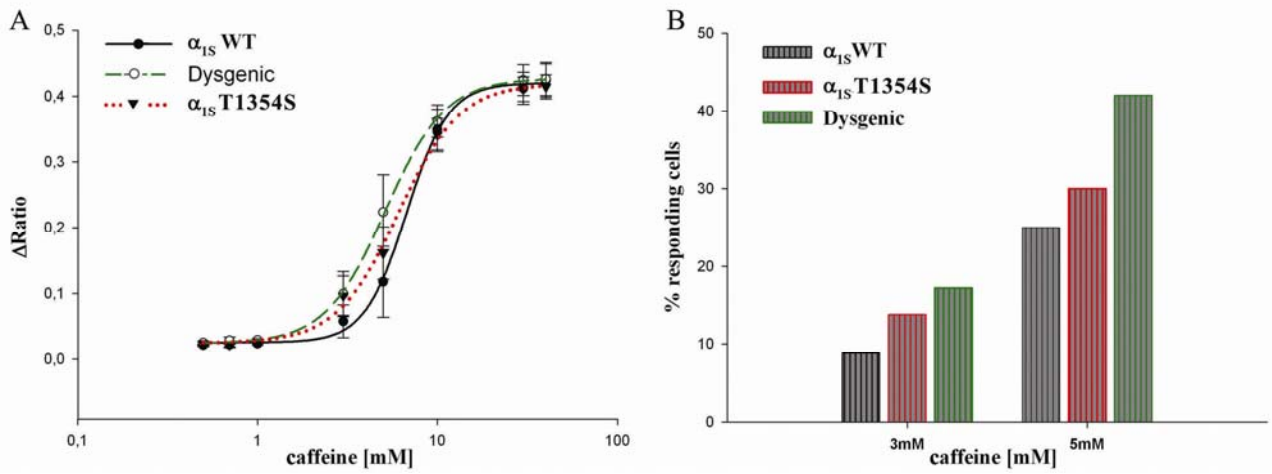

Fig. 20. Caffeine dose-response curves in the MDG expression system. Each point represents the average of maximal caffeine-responses, relative to the baseline taken immediately before every caffeine application. The threshold for caffeine-induced Ca^{2+} release was slightly lower for α_{1S}T1354S-expressing than for α_{1S}WT-expressing myotubes (A). The frequency of responding cells to the threshold caffeine concentrations, 3 and 5 mM was graduated: untransfected dysgenic > α_{1S}T1354S-expressing > α_{1S}WT-expressing myotubes (B).

Effects of additional Ca^{2+} influx through a fast activating Ca^{2+} channel?

As mentioned above, L-type Ca^{2+} currents revealed an accelerated activation for α_{1S}T1354S channels in response to 200ms depolarization steps in whole-cell patch clamp experiments. Now it was of interest, if a faster activating Ca^{2+} channel could have any physiological effects on the intracellular Ca^{2+} concentration and thus, consequently, might influence the Ca^{2+} sensitive RyR1. The integral of the area under the maximal L-type Ca^{2+} current trace (30-40mV potentials) during the initial phase of depolarization gives an estimation of the Ca^{2+} influx in this specific time-period. The Ca^{2+} influx taken from the first 20ms of depolarization resulted in considerably higher values for α_{1S}T1354S currents compared to WT (Fig.21A, B). To even enhance the putative effects of an accelerated Ca^{2+} influx, a new, high conductive (hc) control construct, α_{1S}hc, was introduced in the experimental plans. The α_{1S}hc-subunit is a splice variant of α_{1S} that showed in patch clamp recordings accelerated activation and high Ca^{2+} conductivity, approximately 7-8 times higher than Ca^{2+} currents measured from α_{1S} WT expressing myotubes. Ca^{2+} influx, in the first 5-20ms of the depolarization step (with rather the shorter time frames mirroring a skeletal muscle action potential) resulted in distinct values at all time frames with a continuous graduation of α_{1S}WT < α_{1S}T1354S < α_{1S}hc (Fig.21C).

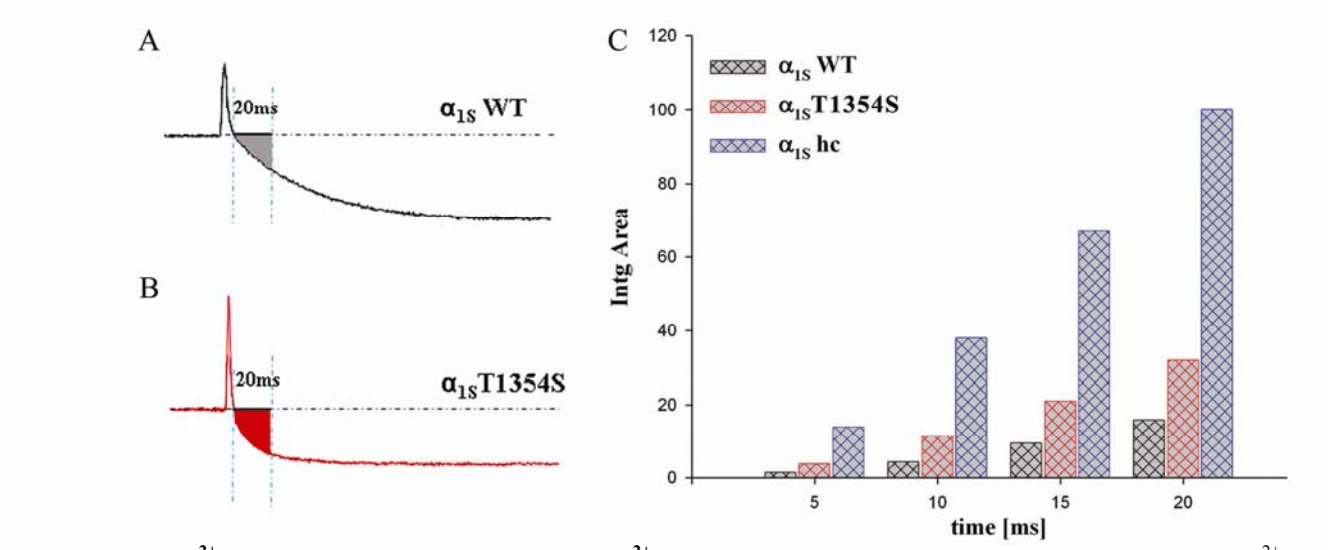

Fig. 21. Ca^{2+} influx in slow and fast activating Ca^{2+} channels. The integral of the area under the maximal Ca^{2+} trace shows an increased Ca^{2+} influx in the first 20 ms of depolarization through α_{1S}T1354S channels compared to WT channels (A, B). Ca^{2+} influx was even higher for the α_{1S}hc control construct (C).

To test whether this additional Ca^{2+} influx observed in fast activating channels could affect the intracellular Ca^{2+} concentration and thus intracellular Ca^{2+} transients, Ca^{2+} release via RyR1 was evoked by extracellular electrical field stimulation. Electrical pulse train application is easy to control and it is possible to modify the frequency, the number of pulses, the duration and the intensity of each pulse. In the field stimulation protocol designed for a first run, transfected MDG myotubes were stimulated with three 10V * 2ms pulses at 0.3Hz followed by a pulse train of 20Hz * 2s (Fig. 22A) to sum up the putative Ca^{2+} effects in this tetanic stimulation. This stimulation train was repeated during a sequential exposition to 0, 1 and 2mM caffeine solution prepared in Ringer with addition of 2 or 10mM Ca^{2+}. Each application was followed by 60-s washes with Ringer solution without caffeine. Under this tetanic stimulation protocol, no differences in Ca^{2+} release between α_{1S}WT and α_{1S}T1354S-expressing solutions (Fig. 22C).

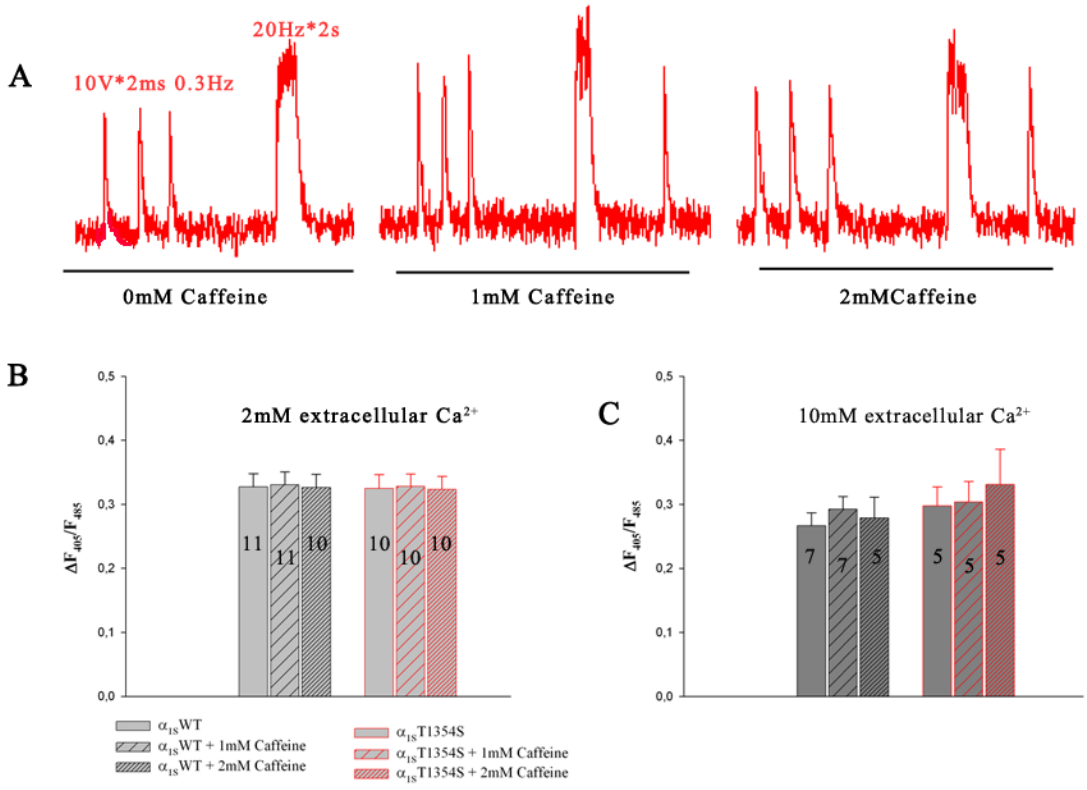

Fig. 22. High frequency field stimulation. MDG cells were stimulated with short pulses (10V * 2ms) and with a tetanic pulse at 20Hz * 2s (A). No differences in SR Ca^{2+} release under tetanic stimulation were observed (measured as the plateau of the tetanus ± SE) in 2mM and 10mM extracellular Ca^{2+}, respectively (B, C). Numbers of recordings are indicated inside the columns.

Considering that high stimulation frequency might not have been the appropriate tool to distinguish the effects of elevated Ca^{2+} influx on the SR Ca^{2+} release, the frequency of the tetanic stimulation was reduced to 5Hz for a new series of measurements, performed in extracellular solutions containing 10mM Ca^{2+}.

Again, no differences were observed in Ca^{2+} release after application of tetanic stimulation, comparing α_{1S}WT, α_{1S}T1354S and α_{1S}hc-expressing myotubes. However, a change in SR Ca^{2+} release induced by single pulses at 0.3Hz could be identified when comparing α_{1S}WT and the faster activating channels, after perfusing the expressing cells with solutions containing 10mM Ca^{2+} and 1-2mM caffeine (Fig. 23A, B). The integral of the Ca^{2+} release transient peaks (a more accurate measure of Ca^{2+} release than the height of the peak) showed a significant amplification ($P<0.005$) under caffeine perfusion in α_{1S}hc-expressing myotubes compared to α_{1S}WT-expressing myotubes. However, α_{1S}T1354S-expressing myotubes are positioned between these values, and thus show exactly the same tendency (Fig. 23C).

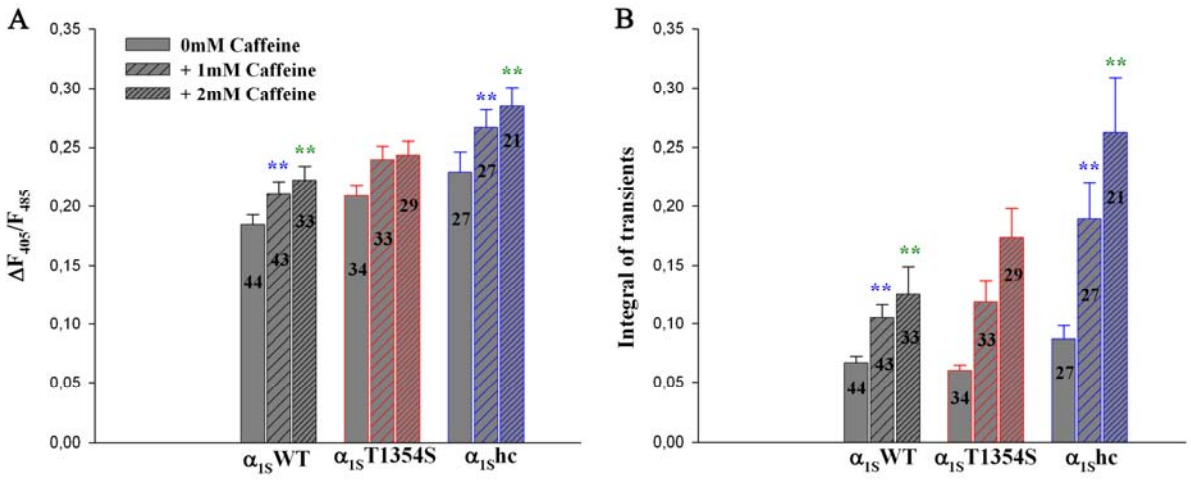

Fig. 23. Low frequency field stimulation. When MDG cells were stimulated at 0.3Hz and at 5Hz, SR Ca^{2+} release induced by single pulses (0.3Hz) was elevated (** $P<0.005$) under 1 and 2mM caffeine in α_{1S}T1354S and α_{1S}hc compared to α_{1S}WT-expressing myotubes. A plot of the height of the Ca^{2+} release peaks ± SE (B) and the integral of the transient peaks ± SE (C) are shown. Numbers of recordings are indicated inside the columns.

To test the hypothesis that extracellular Ca^{2+} influx is responsible for this additional activation of SR Ca^{2+} release under the influence of caffeine, which is especially prominently seen with the higher Ca^{2+}-conducting α_{1S} constructs, field stimulation experiments at low frequency (10V * 2ms at 0.3Hz) were performed during the sequential application of Ca^{2+}-free and 10mM Ca^{2+}-containing external solutions, both in combination with 1 and 2mM of caffeine, respectively (Fig.24).

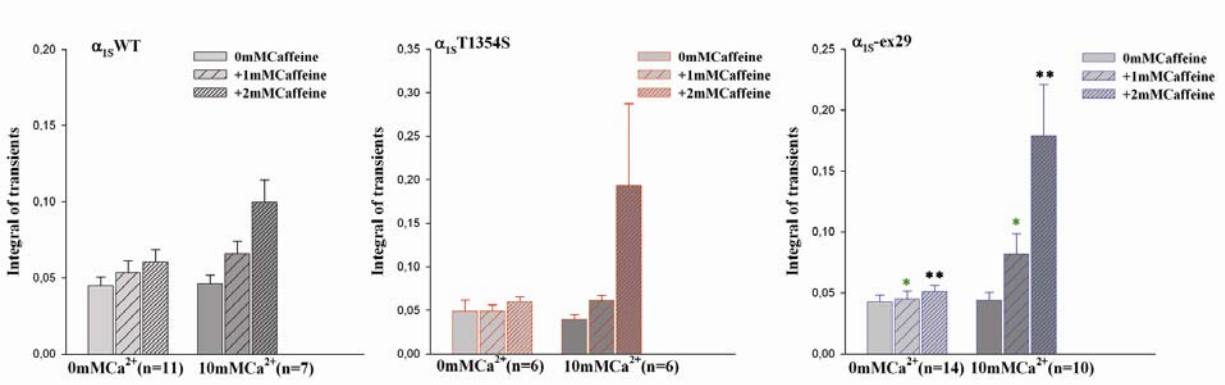

Fig. 24. Field stimulation in 0 and 10mM extracellular Ca^{2+}. Integral of SR Ca^{2+} release ± SE was comparable for all the constructs (α_{1S}WT, α_{1S}T1354S and α_{1S}hc) in 0mM extracellular Ca^{2+} but significantly increased (* $P<0.05$; ** $P<0.005$) in α_{1S}hc in presence of 10mM extracellular Ca^{2+} and 1-2mM of caffeine.

Alternatively, the elevated SR Ca^{2+} release observed in myotubes expressing the fast activating / high conductive Ca^{2+} channels could be due to an elevated SR Ca^{2+} loading or to a more direct effect of the action potential induced Ca^{2+} influx on RyR1 sensitization and thus activation. To investigate the underlying mechanism, MDG cells were incubated for 2min with 10mM Ca^{2+} to allow sufficient SR loading. Subsequently, three electrical pulses (10V * 2ms) were repeatedly applied during a sequential 30sec-exposure to 2mM Ca^{2+} together with either 0, 1 or 2mM caffeine (Fig.25A).

The tendency of an increased SR Ca^{2+} release in α_{1S}T1354S and α_{1S}hc-expressing myotubes compared to α_{1S}WT was found again and resembled the situation without preloading. This effect was even more pronounced during caffeine perfusion (Fig.25B), suggesting that Ca^{2+} influx does primarily not affect SR loading properties but rather interact directly with RyR1 and hence sensitizes SR Ca^{2+} release.

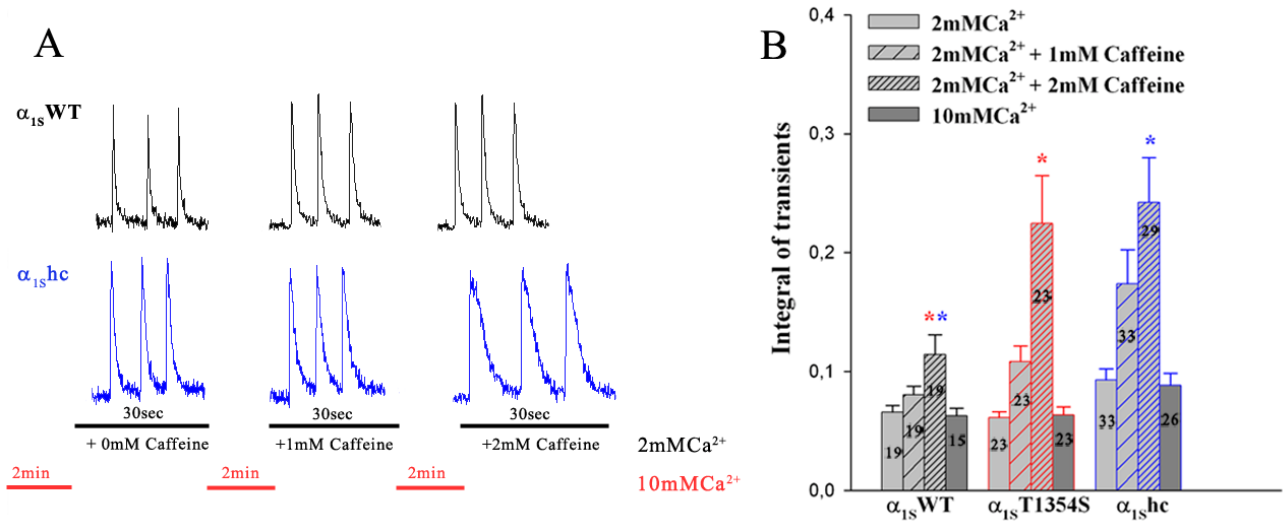

Fig. 25. Field stimulation in 2mM Ca^{2+} after preloading with 10mM Ca^{2+}. Action potential induced Ca^{2+} release in 2mM Ca^{2+} after a 2min preloading period with 10mM Ca^{2+} (A) resulted in more robust Ca^{2+} transient peaks (* $p<0.05$) in α_{1S}T1354S and α_{1S}hc, than in α_{1S}WT-expressing myotubes during caffeine perfusion. Integral of the transient peaks ± SE is shown in (B). Numbers of recordings are indicated inside the columns.

The hypothesis that Ca^{2+} influx enhances the caffeine-induced SR Ca^{2+} release was tested again in a new set of field stimulation experiments, using additionally the non- Ca^{2+}-conductive α_{1S}D396K subunit (courtesy Grabner, Schredelseker, Shrivastav; unpublished construct). The pore loop point mutant α_{1S}D396K, when expressed in GLT myotubes was unable to restore L-type Ca^{2+} currents despite the existence of intracellular Ca^{2+} transients comparable in amplitude and voltage dependence to those in α_{1S}WT-expressing myotubes.

Action potential-induced SR Ca^{2+} release was again recorded in transfected MDG myotubes by applying three single pulses (at 10V * 2ms) during the application of extracellular solutions containing different concentrations of Ca^{2+} and caffeine.The resulting SR Ca^{2+} release was comparable in α_{1S}D396K and α_{1S}WT-expressing myotubes but significantly increased (*$p<0.05$) for the highly conductive channel α_{1S}hc. Again, the α_{1S}T1354S expressing myotubes showed an intermediate response between α_{1S}WT and α_{1S}hc during caffeine application, confirming the previously observed tendency (Fig. 26). These findings provide strong evidence that elevated Ca^{2+} influx through the DHPR-α_{1S} plays a role in the sensitizing of the skeletal muscle RyR1 and thus leads to an activation of Ca^{2+} release.

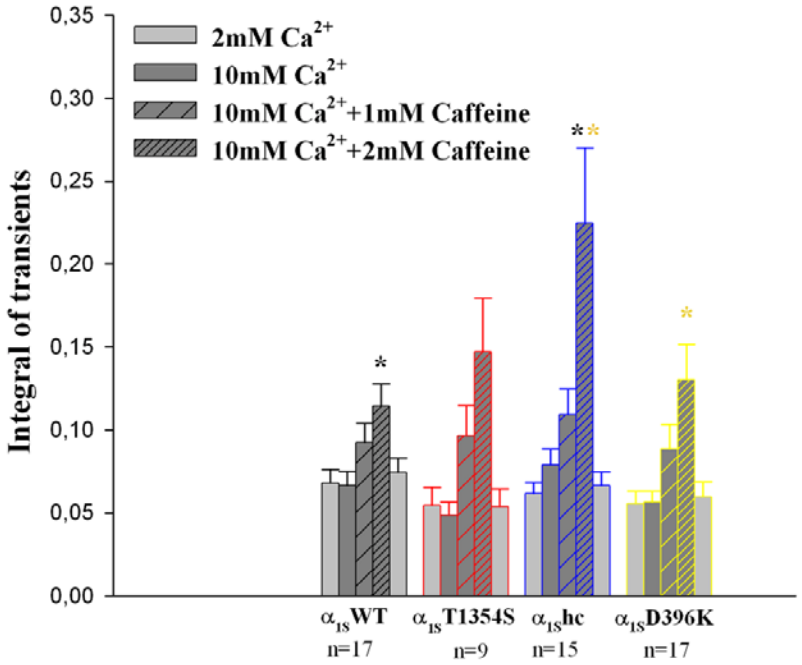

Fig. 26. Field stimulation in α_{1S}D396K expressing MDG myotubes. Action potential induced SR Ca^{2+} release was comparable in α_{1S}D396K and α_{1S}WT-expressing myotubes but higher (*$p<0.05$; *$p<0.06$) in α_{1S}hc expressing myotubes during caffeine applications.

Concluding, we can summarize that the MH-associated α_{1S}T1354S L-type channel mutation is characterized by a faster activation that results in an increased Ca^{2+} influx during the action potential. This additional Ca^{2+} influx together with the higher caffeine sensitivity of Ca^{2+} release, observed in the presence of the point mutant α_{1S}T1354S channel, accounts for increased depolarization-dependent intracellular Ca^{2+} transients that could explain the MH phenotype.

DISCUSSION

MH is a pharmacogenetic disorder of skeletal muscle EC coupling, characterized by an abnormal regulation of Ca^{2+} release from the SR that leads to an increased and non-physiological intracellular Ca^{2+} level. The pathogenic mechanisms of MH, even still not completely and well defined, seems to arise from abandoned Ca^{2+} release due to an increased sensitivity of the SR Ca^{2+} release channels RyR1 to different activating stimuli.

The first studies, made in a porcine model for MH showed an altered Ca^{2+}-induced Ca^{2+} release (CICR) mechanism of SR[46] and an increased sensitivity of RyR1 to halothane, succinylcholine, caffeine and 4-chloro-m-cresol[47,48]. Beside these, also a reduced inhibitory effect of Mg^{2+} and Ca^{2+} has been described to account as well for the altered gating of MH susceptible (MHS) SR channels[49, 50]. In most of the cases, MH susceptibility is associated to mutations in the gene encoding RyR1, but several other genes are also associated to this disorder. However, so far the mutations α_{1S}R1086H[27] and α_{1S}T1354S[28] of the α_{1S} subunit of the DHPR are the only specific MH mutations that have been identified in a protein other than RyR1.

Apart from MH crisis episodes induced upon the exposition to volatile anesthetics or depolarizing muscle relaxants, MHS patients do not show clinically relevant symptoms in normal life. Thus, the single point mutations associated with MHS can not severely affect the muscle physiology but only show rather marginal effects under specific and stringent conditions. In this study we evaluated the functional expression and physiological impact of the recently detected mutant α_{1S}T1354S[28] on SR Ca^{2+} release using different experimental approaches with the combined use of pharmacological stimuli to describe a new pathogenic mechanism of MH.

Normal membrane expression, triad targeting and voltage-sensing in α_{1S}T1354S expressing myotubes.

As previously described, the α_{1S} subunit contains molecular domains for interactions with the

other accessory subunits [9] of the DHPR and with the RyR1[5]. Thus, it was important to verify whether point mutation T1354S could affect the membrane expression of the α_{1S} subunit and consequently the correct muscle-specific arrangement of DHPR and RyR1.

As shown in Fig.8, the immunocytochemistry analysis proved the correct expression and distribution of α_{1S}T1354S in clusters that perfectly colocalized with RyR1 clusters. This means that the point mutation T1354S does not affect the correct location of the two channels in junctions of the SR with the plasma membrane (peripheral couplings) or with the T-tubules (triadic couplings), which is a prerequisite for the physical DHPR-RyR1 interaction. Second, and most important for muscle physiology, was to test the effect of mutation T1354S on skeletal muscle EC coupling. Skeletal muscle DHPRs play a pivotal role in the process by which depolarization of the sarcolemma causes the release of Ca^{2+} from the SR, ultimately resulting in muscle contraction. Skeletal muscle DHPRs are low conductance L-type Ca^{2+} channels[51] that are characterized by slow activation kinetics, requiring more than 100 ms to open fully[52]. Therefore, L-type Ca^{2+} currents in whole-cell patch clamp experiments are elicited by 200ms depolarization steps.

In contrast to the previously described and characterized MH mutant α_{1S}R1086H[42], where the L-type current density was reduced and the voltage gated Ca^{2+} release activated at more negative voltages, in α_{1S}T1354S-expressing myotubes the amplitudes and voltage dependence of L-type Ca^{2+} currents and Ca^{2+} transients in response to 200ms depolarization step were indistinguishable from those of α_{1S}WT-expressing myotubes (Fig.9). As skeletal muscle DHPRs are understood to act mainly as voltage sensors for EC coupling by providing a mechanical link between sarcolemmal depolarization and the release of Ca^{2+} from the SR, we concluded that the mutation T1354S does not affect the voltage sensor function of the α_{1S}.

However, the finding that the T1354S mutation in DHPR-α_{1S} did not enhance the sensitivity of the Ca^{2+} release to activation by the endogenous stimulus (depolarization) did not exclude the possibility that it could affect the Ca^{2+} release upon activation with a pharmacological activator of RyR1 (i.e. caffeine). To test this hypothesis, we measured L-type Ca^{2+} currents and Ca^{2+} transients in response to 200ms depolarization step in the absence and presence of 2mM caffeine. No difference was found in voltage-dependence and amplitude between the α_{1S}WT

and α_{1S}T1354S-expressing myotubes even in presence of caffeine (Fig.13). Nevertheless, action potential-induced Ca^{2+} transients measured in presence of 1 and 2mM caffeine resulted to be higher in α_{1S}T1354S compared to α_{1S}WT-expressing myotubes (Fig.23). These results indicate that the mutation T1354S slightly enhanced the sensitivity of Ca^{2+} release to activation by caffeine and that it is not possible to discriminate this minute effect during a long and non-physiological depolarization stimulus of 200ms.

T1354S accelerates Ca^{2+} current kinetics

Although amplitudes and voltage dependence of Ca^{2+} current and Ca^{2+} transients in α_{1S}T1354S-expressing myotubes were similar to the α_{1S}WT control, current kinetics were different. The reduction of the time-to-peak value in the mutant T1354S channel indicated an accelerated activation of Ca^{2+} currents.

Previous studies[9] showed that the Ca^{2+} current kinetics are determined by the $\alpha_2\delta$–1 subunit and that the extracellular regions of α_{1S}- subunits are involved in the interaction with the $\alpha_2\delta$–1subunit[53]. According to these findings and according to our first results showing that the T1354Smutation, located in the IVS5-S6 extracellular P-loop of α_{1S}, accelerates the Ca^{2+} current kinetic, we hypothesized that this T1354S mutation could disturb the interaction between α_{1S} - $\alpha_2\delta$–1subunits. In normal muscle cells there are two populations of Ca^{2+} channel complexes: slow and fast activating channels, respectively, that are understood as existing with and without $\alpha_2\delta$–1 subunits. If mutation T1354S had affected the correct association of $\alpha_2\delta$–1 to $\alpha_{1S,}$ the balance between the two current components would have been altered, with a predominance of the fast activating component. Our kinetic analysis showed that in the mutant α_{1S}T1354S channel, exactly as in the α_{1S}WT, the slow and fast components contributed equally to the total current amplitude (Fig.11). This provides evidence that the T1354S mutation does not disturb the functional interaction of $\alpha_2\delta$–1 and α_{1S} subunits. The same conclusion was drawn from immunocytochemistry, where we observed perfect colocalization of $\alpha_2\delta$–1 and α_{1S} clusters (Fig.12). This was consistent with previously published studies in

which was demonstrated that this is the fact only in normal myotubes, while in dysgenic myotubes the $\alpha_2\delta-1$ subunit is diffusely expressed and mistargeted into the plasma membrane[41].

Even though mutation T1354S obviously does not disturb the balance between the two channel populations, the significantly reduced time constants (τ_{slow} and τ_{fast}) of both the two components in the mutant channel proved that the mutation T1354S affects the intrinsic kinetic properties of the Ca^{2+} channel.

Caffeine sensitivity of RyR1 in α_{1S}T1354S-expressing myotubes

It was previously shown that skeletal muscle from MHS individuals and animals have a lower pharmacological threshold for and an exaggerated response to submaximal concentrations of caffeine[54] and 4-chloro-*m*-cresol (4-CmC)[55] compared to those from MH-nonsusceptible (MHN) subjects. This enhanced sensitivity is widely used as part of the clinical diagnosis of MHS in humans and has been confirmed experimentally in swine[56]. The molecular and cellular basis for enhanced sensitivity to pharmacological agents in MHS has remained unclear. Some evidences suggest that the amplified intracellular Ca^{2+} release at submaximal concentrations of caffeine and 4-CmC is closely associated with the high resting $[Ca^{2+}]_i$ observed in these cells[57]. However, other studies revealed that at rest, before activation, the DHPR exerts a negative long-range allosterism on RyR1, reducing its sensitivity to direct agonists such as caffeine[58]. This hypothesis was also confirmed by *Weiss et al.* proposing that the MH mutation R1086H in the DHPR α_{1S} subunit, located in the III-IV intracellular loop, disrupts this negative DHPR-mediated allosteric regulation of the SR Ca^{2+} release mechanism[42]. Surprisingly, we also found that the threshold for caffeine-induced Ca^{2+} release is slightly lower in α_{1S}T1354S-expressing myotubes compared with that of α_{1S}WT-expressing myotubes and approximates the values obtained from dysgenic myotubes. However, in contrast to the R1086H-expressing myotubes, we did not find elevated resting Ca^{2+} level in α_{1S}T1354S-expressing myotubes[42]. Considering that at threshold concentration (3mM and 5mM) of caffeine a major number of α_{1S}T1354S-

expressing myotubes responded, we could conclude that the MH T1354S mutation also weakens the control mechanism of DHPR-α_{1S} on SR Ca^{2+} release (Fig.20).

The role of increased Ca^{2+} influx and of increased RyR1 caffeine sensitivity on SR Ca^{2+} release

Finally the question arises, whether and how the acceleration of Ca^{2+} channel activation contributes to an increased SR Ca^{2+} release that might account for elevated intracellular Ca^{2+} levels characterizing the MH phenotype, and whether the observed slightly increased caffeine sensitivity of SR Ca^{2+} channels in α_{1S}T1354S-expressing myotubes enhances this effect. Under physiological conditions, a brief action potential (few ms) triggers conformational changes of the DHPR by the gating charge movement of its voltage sensor, which, in turn, activates the RyR1 in the SR to open. L-type currents induced by a long depolarization steps like used in regular patch-clamp protocols (200ms), do not represent the physiological situation in the skeletal muscle cell and the effect of fast activation might be underestimated. In fact, if we consider the integral of the area in the first 5-20ms of the maximal L-type Ca^{2+} current traces we can estimate a higher Ca^{2+} influx through the faster activating channels compared to the control. This difference is no more evident when integrating the area of the maximal L-type Ca^{2+} current traces over the full 200ms period. On this finding, the next question was, whether this additional Ca^{2+} influx affects the SR Ca^{2+} release mechanism and whether it is enhanced in presence of low concentrations of caffeine. A this point, expecting that the effects of a MH point mutation on Ca^{2+} channel activity is rather tiny and marginal, and thus can not be easily discriminated and evaluated, we introduced in our experimental plans an additional α_{1S} construct (α_{1S}hc), characterized by robustly increased Ca^{2+} conductivity (circa 8-fold higher than the α_{1S}WT subunit) and accelerated activation. Thus, subunit α_{1S}hc was expected to enhance the hypothesized effects of the α_{1S}T1354S subunit on the SR Ca^{2+} release mechanism and hence support the evidence that the acceleration of the Ca^{2+} channel activation contributes to a higher Ca^{2+} influx. And indeed, in field stimulation experiments at low frequency (0.3Hz) and 10mM extracellular Ca^{2+} solution, we could find higher action potential-induced Ca^{2+}

release in α_{1S}T1354S and α_{1S}hc-expressing myotubes than in those expressing α_{1S}WT. This effect was even more pronounced in the presence of low caffeine-concentrations. In accordance to our working hypothesis that Ca^{2+} influx plays a role, even marginal, on the SR Ca^{2+} release, we should expect in Ca^{2+}-free extracellular solutions no differences in action potential-induced Ca^{2+} release between normal and faster activating Ca^{2+} channels. And this was exactly what we observed (Fig. 24). Surprisingly, in Ca^{2+}- free solutions even the caffeine effect on Ca^{2+} release was no more evident. However, this can again be judged as a prove that extracellular Ca^{2+} has a profound effect on caffeine-induced Ca^{2+} release and on SR Ca^{2+} stores[59]. Finally, by Ca^{2+} pre-filling of the SR stores[60] (Fig.25) we could demonstrate, that additional Ca^{2+} influx has rather a direct effect on RyR1 activation and does not affect the SR loaded state. In all our experiments we could continuously observe increased electrically-induced Ca^{2+} release in α_{1S}T1354S and α_{1S}hc-expressing myotubes during the application of Ca^{2+} and caffeine, suggesting a concerted effect of Ca^{2+} influx and caffeine on the activation of RyR1. An additional concept to confirm the Ca^{2+} free recording results with the consequential changes in SR Ca^{2+} release in presence of 1 and 2mM caffeine, would have been to block the DHPR channels either with La^{3+} and Cd^{2+} or with the organic DHPR blocker nifedipine. Unfortunately, these DHPR blockers increase the sensitivity of RyR1 to caffeine[61]. Thus, the only additional way to examine again the combined effect of Ca^{2+} influx and caffeine on the activation of RyR1 was to use a non-conductive α_{1S} subunit (α_{1S}D396K). The comparable Ca^{2+} release in α_{1S}D396K and α_{1S}WT-expressing myotubes (Fig.26) proved again our hypothesis of a concerted mechanism of Ca^{2+} influx and caffeine on SR Ca^{2+} release. Taken together, the evidence provided here suggests that in myotubes expressing the MH α_{1S}T1354S mutant the additional Ca^{2+} influx, due to the accelerated kinetics of the Ca^{2+} channels together with higher caffeine sensitivity of RyR1, accounts for an increased intracellular Ca^{2+} level that could explain the MH phenotype by a hitherto unnoticed mechanism.

Acknowledgments

The work presented here was made during my PhD program in "Genetica e Medicina Molecolare" of the University of Napoli "Federico II" from 2003 to 2007. The project started in the Department of "Biochimica Clinica e Biotecnologie Mediche" at University of Napoli in the lab of Prof. Francesco Salvatore and Prof. Antonella Carsana and continued in the Division of Biochemical Pharmacology at Innsbruck Medical University in the lab of Prof. Manfred Grabner. Although the difficulties, it was a pleasant work and unforgettable experience and for this I have to thank all people who supported me in this years.

First of all **Prof. Francesco Salvatore** and **Prof. Antonella Carsana** to offer me the possibility to continue and conclude a project already started during my degree thesis. Their support was precious to start and keep the collaboration with Innsbruck Medical University and to effort all the costs related to the experimental work.

My thanks go to the Division of Biochemical Pharmacology at Innsbruck Medical University to have welcomed and offered me every help. Anyway my special thanks go to **Manfred Grabner** for being everyday friendly present in the last three years. I found in him a great scientist besides a dear friend with strong temperament and optimism that was essential during this hard but extremely gratifying project. I am very grateful to my **colleagues: Johann Schredelseker** for supporting me in all the experiments, **Sandra Schleret, Manisha Shrivastav** and **Anamika Dayal**: all of them make every working day more easy and enjoyable. Thanks to **Berhard Flucher, Petronel Tuluc** and **all their lab coworkers** for their continuous scientific contributes and also for relaxing and fun moments. The success of this work is due also to the daily and constant support of my **family**, my **brother** and my **boyfriend**. And finally thanks to **all my friends** in Innsbruck for sharing nice moments in the free time and all my **friends and colleagues in Napoli** to blunt my homesickness. The project was supported by MIUR, CEINGE and Der Wissenschaftsfonds.

References

[1]**Adams BA, Tanabe T, Mikami A, Numa S, Beam KG** (1990). Intramembrane charge movement restored in dysgenic skeletal muscle by injection of dihydropyridine receptor cDNAs. *Nature* 346 (6284):569-72.

[2]**Bezanilla F.** The voltage sensor in voltage-dependent ion channels (2000). *Physiol Rev* 80(2):555-92.

[3]**Yang J, Ellinor PT, Sather WA, Zhang JF, Tsien RW** (1993). Molecular determinants of Ca^{2+} selectivity and ion permeation in L-type Ca^{2+} channels. *Nature* 366 (6451):158-61.

[4]**De Waard M, Scott VES, Pragnell M, Campbel KP** (1996). Identification of critical amino acids involved in α_1-β interaction in voltage-dependent Ca^{2+} channels. *FEBS Lett* 380: 272-276

[5]**Pragnell M, De Waard M, Mori Y, Tanabe T, Snutch TP, Campbell KP** (1994). Calcium channel beta-subunit binds to a conserved motif in the I-II cytoplasmic linker of the alpha 1-subunit. *Nature* 368: 67-70.

[6]**Grabner M, Dirksen RT, Suda N, Beam KG** (1999)**.**The II-III loop of the skeletal muscle dihydropyridine receptor is responsible for the Bi-directional coupling with the ryanodine receptor. *J Biol Chem* 274(31):21913-9.

[7]**Gregg RG, Messing A, Strube C, Beurg M, Moss R, Behan M, Sukhareva M, Haynes S, Powell JA, Coronado R, Powers PA** (1996). Absence of the beta subunit (cchb1) of the skeletal muscle dihydropyridine receptor alters expression of the alpha 1 subunit and eliminates excitation-contraction coupling. *Proc Natl Acad Sci U S A* 93(24):13961-6.

[8]**Schredelseker J, Di Biase V, Obermair GJ, Felder ET, Flucher BE, Franzini-Armstrong C, Grabner M** (2005).The beta 1a subunit is essential for the assembly of dihydropyridine-receptor arrays in skeletal muscle. *Proc Natl Acad Sci U S A* 102(47):17219-24.

[9]**Obermair GJ, Kugler G, Baumgartner S, Tuluc P, Grabner M, Flucher BE (**2005)**.** The Ca^{2+} channel alpha2delta-1 subunit determines Ca^{2+} current kinetics in skeletal muscle but not targeting of alpha1S or excitation-contraction coupling. *J Biol Chem* 280(3):2229-37.

[10]**Arikkath J, Chen CC, Ahern C, Allamand V, Flanagan JD, Coronado R, Gregg RG, Campbell KP** (2003). γ_1 subunit interactions within the skeletal muscle L-type voltage-gated calcium channels. *J Biol Chem* 278:1212–1219.

[11]**Ursu D, Schuhmeier RP, Freichel M, Flockerzi V, Melzer W** (2004). Altered Inactivation of Ca^{2+} Current and Ca^{2+} Release in Mouse Muscle Fibers Deficient in the DHP receptor gamma1 subunit. *J Gen Physiol* 124:605–618.

[12]**Takeshima H, Nishimura S, Matsumoto T, Ishida H, Kangawa K, Minamino N, Matsuo H, Ueda M, Hanaoka M, Hirose T** (1989)**.** Primary structure and expression from complementary DNA of skeletal muscle ryanodine receptor. *Nature* 339(6224):439-45.

[13]**Fabiato A, Fabiato F** (1978)**.** Calcium-induced release of calcium from the sarcoplasmic reticulum of skinned cells from adult human, dog, cat, rabbit, rat, and frog hearts and from fetal and new-born rat ventricles. *Ann N Y Acad Sci* 307:491-522.

[14]**Armstrong CM, Bezanilla FM, Horowicz P** (1972). Twitches in the presence of ethylene glycolbis(-aminoethyl ether)-N,N'-tetracetic acid*. Biochim Biophys Acta* 267(3):605-8.

[15]**García J, Beam KG** (1994)**.** Measurement of calcium transients and slow calcium current in myotubes. *J Gen Physiol* 103(1):107-23.

[16]**Lu X, Xu L, Meissner G** (1994). Activation of the skeletal muscle calcium release channel by a cytoplasmic loop of the dihydropyridine receptor. *J Biol Chem* 269(9):6511-6.

[17]**Block BA, Imagawa T, Campbell KP, Franzini-Armstrong C** (1988)**.** Structural evidence for direct interaction between the molecular components of the transverse tubule/sarcoplasmic reticulum junction in skeletal muscle. *J Cell Biol* 107:2587-2600.

[18]**Protasi F, Franzini-Armstrong C, Allen PD (**1998)**.** Role of Ryanodine Receptors in the Assembly of Calcium Release Units in Skeletal Muscle. *J. Cell Biol* 140 (4) 831-84.

[19]**Schneider MF, and Chandler WK** (1973). Voltage dependent charge movement in skeletal muscle: a possible step in excitation-contraction coupling. *Nature* 242: 244-246.

[20]**Rosenberg H, Davis M, James D, Pollock N, Stowell K** (2007). Malignant hyperthermia. *Orphanet J Rare Dis* 2:21.

[21]**Ording H, Brancadoro V, Cozzolino S, Ellis FR, Glauber V, Gonano EF, Halsall PJ, Hartung E, Heffron JJ, Heytens L, Kozak-Ribbens G, Kress H, Krivosic-Horber R, Lehmann-Horn F, Mortier W, Nivoche Y, Ranklev-Twetman E, Sigurdsson S, Snoeck M, Stieglitz P, Tegazzin V, Urwyler A, Wappler F** (1997)**.** In vitro contracture test for diagnosis of malignant hyperthermia following the protocol of the European MH Group: results of testing patients surviving fulminant MH and unrelated low-risk subjects. *Acta Anaesthesiol Scand* 41(8):955-66.

[22]**Urwyler A, Deufel T, McCarthy T, West S** (2001). Guidelines for molecular genetic detection of susceptibility to malignant hyperthermia. *Br J Anaesth* 86: 283–7.

[23]**MacLennan DH, Duff C, Zorzato F, Fujii J, Phillips M, Korneluk RG, Frodis W, Britt BA, Worton RG** (1990). Ryanodine receptor gene is a candidate for predisposition to malignant hyperthermia. *Nature* 343 (6258):559-61.

[24]**Healy JM, Lehane M, Heffron JJ, Farrell M, Johnson K, McCarthy TV** (1990). Localization of the malignant hyperthermia susceptibility locus to human chromosome 19q12-q13.2. *Biochem Soc Trans* 18 (2):326.

[25]**McCarthy TV, Quane KA, Lynch PJ** *(2000).* Ryanodine receptor mutations in malignant hyperthermia and central core disease. *Hum Mutat* 15(5):410-7. Review.

[26]**Iles DE, Segers B, Heytens L, Sengers RC, Wieringa B** (1992). High-resolution physical mapping of four microsatellite repeat markers near the RYR1 locus on chromosome 19q13.1 and apparent exclusion of the MHS locus from this region in two malignant hyperthermia susceptible families. *Genomics* 14(3):749-54.

[27]**Monnier N, Procaccio V, Stieglitz P, Lunari J** (1997). Malignant hyperthermia susceptibility is associated with a mutation of α1subunit of human DHPR in skeletal muscle. *Am J Hum Genet* 60:1316-25.

[28]**Pirone A** (2003). Eterogeneita' genetica dell'ipertermia maligna ed analisi di mutazioni e polimorfismi del gene codificante la subunita' alfa-1 del recettore della diidropiridina. *Master thesis, University of Naples.*

[29]**Illes DE, Lehmann F, Scherer SV, Olde Weghuis D, Suijkerbuijk RF, Heytens L, Mikala G, Schwartz A, Ellis FR, Stewart A, Deufel T, Wieringa B** (1994). Localization of the gene encoding the α2/δ subunits of the L-type voltage dependent channel to chromosome 7q and analysis of the segregation of flanking markers in MH susceptible families. *Hum Mol Genet* 3: 969-975.

[30]**Levitt R, Olckers A, Meyers S, Fletcher J E, Rosemberg H, Isacs H, Meyers DA** (1992). Evidence for the localization of a malignant hyperthermia susceptibility, locus (MHS2) to human chromosome 17q. *Genomics* 14: 562-566.

[31]**Sudbrak R, Procaccio V, Curran J** (1995). Mapping of a further MH susceptibility *locus* to chromosome 3q 13.1. *Am J Hum Genet* 56:684-691.

[32] **Robinson R L, Monnier N, Wolz W, Jung M, Reis A, Nuernberg G, Curran J L, Monsieurs KA** (1997). Genome wide search for susceptibility loci in three european malignant hyperthermia pedigrees. *J Hum Genet* 6:935-961.

[33]**Klaus MM, Scordilis SP, Rapalus JM, Briggs RT, Powell JA** (1983). Evidence for dysfunction in the regulation of cytosolic Ca^{2+} in excitation-contraction uncoupled dysgenic muscle. *Dev Biol* 99(1):152-65.

[34]**Powell JA, Petherbridge L, Flucher BE** (1996). Formation of triads without the dihydropyridine receptor alpha subunits in cell lines from dysgenic skeletal muscle. *J Cell Biol* 134(2):375-87.

[35]**Felder E, Protasi F, Hirsch R, Franzini-Armstrong C, Allen PD** (2002). Morphology and molecular composition of sarcoplasmic reticulum surface junctions in the absence of DHPR and RyR in mouse skeletal muscle. *Biophys J* 82(6):3144-9.

[36]**Rando TA, Blau HM** (1994). Primary mouse myoblast purification, characterization and transplantation for cell-mediated gene therapy. *J Cell Biol* 125(6):1275-87.

[37]**Grabner M, Dirksen RT, and Beam KG** (1998). Tagging with green fluorescent protein reveals a distinct subcellular distribution of L-type and non-L-type Ca^{2+} channels expressed in dysgenic myotubes. *Proc Natl Acad Sci U S A* 95(4):1903-8.

[38]**O'Neill SC, Donoso P, and Eisner DA** (1990). The role of $[Ca^{2+}]_i$ and $[Ca^{2+}]$ sensitization in the caffeine contracture of rat myocytes: measurement of $[Ca^{2+}]_i$ and $[caffeine]_i$. *J Physiol* 425:55-70.

[39]**Flucher BE, Andrews SB, Daniels MP** (1994). Molecular organization of transverse tubule/sarcoplasmic reticulum junctions during development of excitation-contraction coupling in skeletal muscle. *Mol Biol Cell* 5(10):1105-18.

[40]**Obermair GJ, Kugler G, Baumgartner S, Tuluc P, Grabner M, Flucher BE** (2005). The Ca^{2+} channel alpha2delta-1 subunit determines Ca^{2+} current kinetics in skeletal muscle but not targeting of alpha1S or excitation-contraction coupling. *J Biol Chem*. 280 (3):2229-37.

[41]**Flucher BE, Phillips JL, Powell JA** (1991)**.** Dihydropyridine receptor alpha subunits in normal and dysgenic muscle in vitro: expression of alpha 1 is required for proper targeting and distribution of alpha 2. *J Cell Biol* 115(5):1345-56.

[42]**Weiss RG, O'Connell KMS, Flucher BE, Allen PD, Grabner M, Dirksen RT** *(2004)***.** Functional analysis of the R1086H malignant hyperthermia mutation in the DHPR reveals an unexpected influence of the III-IV loop on skeletal muscle EC coupling. *Am J Physiol Cell Physiol* 287(4):C1094-102.

[43]**Lopez JR, Contreras J, Linares N, and Allen PD** (2000)**.** Hypersensitivity of malignant hyperthermia-susceptible swine skeletal muscle to caffeine is mediated by high resting myoplasmic Ca^{2+}. *Anesthesiology* 92(6):1799-806.

[44]**Kern G, Flucher BE (***2005)***.** Localization of transgenes and genotyping of H-2kb-tsA58 transgenic mice. *Biotechniques* 38(1):38, 40, 42.

[45]**Felder E, Protasi F, Hirsch R, Franzini-Armstrong C, Allen PD** (2002)**.** Morphology and molecular composition of sarcoplasmic reticulum surface junctions in the absence of DHPR and RyR in mouse skeletal muscle. *Biophys J* 82(6):3144-9.

[46]**Mickelson JR, Ross JA, Reed BK, and Louis CF** (1986). Enhanced Ca^{2+}-induced calcium release by isolated sarcoplasmic reticulum vesicles from malignant hyperthermia susceptible pig muscle. *Biochim Biophys Acta* 862: 318-328.

[47]**Ohnishi ST, Taylor S, and Gronert GA** (1983)**.** Calcium-induced Ca^{2+} release from sarcoplasmic reticulum of pigs susceptible to malignant hyperthermia. The effects of halothane and dantrolene. *FEBS Lett* 161:103-107.

[48]**Richter M, Schleithoff L, Deufel T, Lehmann-Horn F, and Herrmann-Frank A** (1997)**.** Functional characterization of a distinct ryanodine receptor mutation in human malignant hyperthermia-susceptible muscle. *J Biol Chem* 272:5256-2560.

[49]**Fill M, Coronado R, Mickelson JR, Vilven J, Ma JJ, Jacobson BA, and Louis CF** (1990). Abnormal ryanodine receptor channels in malignant hyperthermia*. Biophys J* 57: 471-475.

[50]**Laver DR, Owen VJ, Junankar PR, Taske NL, Dulhunty AF, and Lamb GD** (1997). Reduced inhibitory effect of Mg^{2+} on ryanodine receptor-Ca^{2+} release channels in malignant hyperthermia*. Biophys J* 73: 1913-1924.

[51]**Dirksen RT, Beam KG** (1995). Single calcium channel behavior in native skeletal muscle. *J Gen Physiol* 105: 227-247.

[52]**Tanabe T, Beam KG, Adams BA, Niidome T, Numa S** (1990). Regions of the skeletal muscle dihydropyridine receptor critical for excitation-contraction coupling. *Nature* 346:567-569.

[53]**Gurnett GA**, **Felix R, Campbell K P (**1997). Extracellular Interaction of the Voltage-dependent Ca^{2+} Channel a2d and a1S Subunits. *J Biol Chem* 272(29):18508-12.

[54]**Tong J, Oyamada H, Demaurex N, Grinstein S, McCarthy TV, and MacLennan DH** (1997). Caffeine and halothane sensitivity of intracellular Ca^{2+} release is altered by 15 calcium release channel (ryanodine receptor) mutations associated with malignant hyperthermia and/or central core disease. *J Biol Chem* 272:26332-2633.

[55]**Wehner M, Rueffert H, Koenig F, Neuhaus J, and Olthoff D** (2002)**.** Increased sensitivity to 4-chloro-m-cresol and caffeine in primary myotubes from malignant hyperthermia susceptible individuals carrying the ryanodine receptor 1 Thr2206Met (C6617T) mutation. *Clin Genet* 62:135-146.

[56]**Jurkat-Rott K, McCarthy T, and Lehmann-Horn F** (2000). Genetics and pathogenesis of malignant hyperthermia. *Muscle Nerve* 23:4-17.

[57]**López JR**, **Contreras J**, **Linares N**, **Allen PD** (2000). Hypersensitivity of malignant hyperthermia-susceptible swine skeletal muscle to caffeine is mediated by high resting myoplasmic [Ca^{2+}]. *Anesthesiology* 92(6):1799-1806.

[58]**Lee EH, Lopez JR, Li J, Protasi F, Pessah IN, Kim DH, Allen PD** (2004). Conformational coupling of DHPR and RyR1 in skeletal myotubes is influenced by long-range allosterism: evidence for a negative regulatory module. *Am J Physiol Cell Physiol* 286(1):C179-89.

[59]**Tong J, McCarthy TV, MacLennan DH** (1999). Measurement of resting cytosolic Ca^{2+} concentrations and Ca^{2+} store size in HEK-293 cells transfected with malignant hyperthermia or central core disease mutant Ca^{2+} release channels. *J Biol Chem* 274 (2):693-702.

[60]**Kurebayashi N, Ogawa Y** (2001). Depletion of Ca^{2+} in the sarcoplasmic reticulum stimulates Ca^{2+} entry into mouse skeletal muscle fibres. *J Physiol* 533(Pt 1):185-99.

[61]**Weigl LG, Hohenegger M, and Kress HG** (2000). Dihydropyridine-induced Ca^{2+} release from ryanodine-sensitive Ca^{2+} pools in human skeletal muscle cells. *J Physiol* 525(Pt 2):461-9.